ANNUAL REPORT

Jan. 1997 – Dec. 1997

of the MSU group to LIGO project

SUSPENSIONS AND SUSPENSION NOISE FOR LIGO TEST MASSES

NSF Grant PHY-9503642.

CONTRIBUTORS: V.B.Braginsky (P.I.)

I.A.Bilenko

M.L.Gorodetsky

F.Ya.Khalili

V.P.Mitrofanov

K.V.Tokmakov

S.P.Vyatchanin

students:

A.Yu.Ageev

I.A.Elkin

N.A.Styazhkina

Contents

I. SUMMARY

A. The investigation of excess noise in violin modes of steel wires

During the year 1997 a new set of records of the mechanical vibrations of violin modes was obtained. In contrast with the former measurements of 1996 of the excess noise observed above the Brownian motion in $20\,\mu m$ diameter tungsten wires we have tested now the noise in $80\mu m$ steel wires made of the same material that is used in LIGO prototype. As we expected smaller mean square amplitude of the Brownian motion due to the larger diameter of the wires, we had to improve substantially the optical readout system. The achieved new resolution $2 \times 10^{-11} cm/\sqrt{Hz}$ was sufficient to record Brownian vibration with relative accuracy better than 10% (see details in Appendix I).

The main results of these measurements are the following:

1. We observed the existence of two types of excess noise: the first is relatively rare rises and falls of the mean amplitude over several relaxation times; the second is presence of fast variations (jumps) of the amplitude with the event rate higher as compared to pure Brownian motion.

2. The total intensity and amplitude of the excess noise peaks were remarkably (5-8 times) lower than in case of tungsten wires.

3. We have not observed significant dependence of the excess noise on the stress value within the range of applied loads (see details in Appendix I).

B. Design and development of a new vacuum chamber for the tests of Q-factors in suspension's modes

In our attempts to obtain high mechanical Q-factors in the suspensions' modes (see annual MSU reports 1995 and 1996) we have reached $Q_{viol} \simeq (0.5 \div 1.1) \times 10^8$ and $Q_{pend} \simeq 1 \times 10^8$. In those experiments it is likely that the obtained values are not the ultimate

ones for a very pure fused silica suspension because of the substantially large gap between precalculated and the measured values. The origin of the discrepancy was probably due to the insufficient depression of some sources of dissipation (recoil losses, residiual gas losses, surface losses in suspension fibers, electric field losses). These main motivations were the basic ones which led us to ellaboration of a new design and implementation of a new vacuum chamber. We expect to obtain higher quality factors first of all in pendulum modes. During 1997 the design was done and a chamber with the installation attached to a heavy basement wall were manufactured, assembled and tested. The obtained vacuum is 3×10^{-8} Torr (in older chamber it was only 2×10^{-6} Torr). At present installation of special inchamber equipment is in progress. The first tests of losses in new suspension may be realized in coming spring. (See details in Appendix II).

C. The investigation of dynamical and dissipative actions of electric controller on the test mass

It is reasonable to expect that the usage of an electric controller will produce dynamical and dissipative actions on the test masses (although these actions will be much smaller than that from a magnetic actuator). In our previous preliminary experiments we observed the dissipative actions on the test masses due to the following processes:

1. the dissipative processes on the surface of conductors which are connected to the source of electrical field;

2. electrostatic field produced by electrical charges located on the surface of fused silica;

3. Joule losses in resistive part of the controller cirquit.

To obtain the complete necessary information about the role of the processes 1. and 2. and about the possibilities to decrease their dynamical and dissipative actions it is necessary to rearrange inchamber equipment and to make some changes in the chamber itself. This will be done next spring.

In this report we describe the results we obtained about the source 3. The main result of the described in Appendix III measurements and calculations is that this source does not prevent to obtain $Q \geq 10^8$ when the controller tunes the test mass at a distance of the order of 10^{-5} cm. (See details in Appendix III)

D. The analysis of a new principle of intracavity readout system

In 1997 a new intracavity readout system was proposed and analysed. In brief the principle of this scheme is the following. Let in the system the two coupled Fabry-Perot resonators initially be identical. Small variations of its lengths lead to amplified redistribution of energy causing force on central mirror. The resulting mirror displacement may be detected using methods standard for the bar antennas. The scheme provides gain in resolution and allows to beat the standard quantum limit without the use of non-classical pumping. The origin of this key advantage is that the fluctuations in optical part of the meter may be in principle totally excluded and the only source of back action will be the meter, which in case of microwave transducer consumes very small amount of energy.

The ultimate sensitivity and the required optical pump power in this scheme do not depend on the quantum state of the pump field. The required state of e. m. field in the resonator with a well determined energy difference in the two arms of the antenna is forming automatically in the process of monitoring the coordinate of the coupling mirror. (See details in Appendix IV)

E. New SQL free principle of coordinate monitoring of the test mass

The new concept of quantum measurement — quantum variation measurement — is proposed to circumvent the standard quantum limit with meter for continuous coordinate registration. Heisenberg microscope as a variant of coordinate meter is analyzed. The idea can be clarified on the example of two measurements separated in time and space, using apriori knowledge on duration and form of acting force. In the first measurement the linear

combination of coordinate and back action momentum should be obtained (it is possible for real coordinate meter) and in the second one experimentalist measures the coordinate. The subtractions of the results of these measurements permit to exclude the response on the back action and thus to circumvent the standard quantum limit. These speculations can be extended on procedure of continuous measurement. (See details in Appendix V).

Appendix 1

I. THE MEASUREMENTS OF THE EXCESS NOISE IN THE STEEL SUSPENSION WIRES: TECHNIQUES AND RESULTS.

The laser interferometric device prepared formerly for the excess noise research has been used. An essential improvement of the experimental installation and the method of measurement have been made in comparison with the first one in which the tunsten wires have been examined. The amplitude of Brownian oscillation on the fundamental violin mode of a string is:

$$\bar{A} = \sqrt{\frac{2kT}{m^*\omega^2}} \tag{1}$$

Here ω is violin mode frequency, k is Boltzman constant, T is temperature and m^* is effective mass of the string. For the steel wires $l = 15\ cm$ long and 80 μm in diameter under the stress about 50% of breaking tension value $\omega \simeq 2\pi \times 1.5\ kHz$, $\bar{A} \simeq 2 \times 10^{-10}\ cm$. This value is approximately 3 times smaller than in the previous experiments with the tungsten wires.

We have managed to increase the sensitivity of the measurements up to 20 times and reached the value of displacement resolution

$$\Delta x_{min} \simeq 2 \times 10^{-11}\ cm/\sqrt{Hz} \tag{2}$$

The key feature of the new installation is the possibility of parallel observations on the two different samples placed in the ends of two arms of the interferometer (see *Figure*1). It allows one to vetoe any external disturbances due to residual seismic and laser power fluctuations using an anticorrelation method. In additional, the enhanced feedback stabilization scheme have kept the perfect tuning of the interferometer during up to $10-14$ hours, which allows to make a long time records. A new calibration method has been used. We used the $He-Ne$ laser wavelength as a reference. The beam splitter was attached to PZT drive,

which could be driven by the AC source on the frequency close to the fundamental mode frequencies of the tested wires. When the amplitude of the beam splitter oscillation reaches the quarter wave value, the output signal on this frequency becomes specifically distorted. Reducing the AC value till the response of the system becomes equal to the signals corresponded to the wires oscillations one can determine these amplitudes with sufficient accuracy. At the same time the linearity of the system is tested. In the process of measurements the PZT drive was used by feedback stabilization scheme for the compensation of slow drift in the interferometer.

The noise properties of a steel wire samples has been studied. We tested the material provided by *LIGO* team, identical to the one used for the mirror suspension on the prototype and first stage of the *LIGO* detector.

In this report the results obtained on the steel samples 15 cm length 80 μm in diameter under the stresses from 50% to 95% from the breaking tension value are presented. All the samples had been polished and cleaned before measurement. The breaking tension value has been determined in the set of the preliminary tests as the ratio of the critical load value to the cross-section area of the samples. Critical load cases the break of the samples during 1-3 seconds.

While each sample was fixed on the frame of experimental device once forever, it was still possible to change its stress from one measurement to another. The minimum interval between the measurements was $3-4$ *hours* because this process requires the vacuum chamber to be open. In contrast with the previous experiments with tungsten only the top end of the sample was rigidly clamped. The bottom end was attached to the lead load. To prevent the horizontal movement of the load it was fixed by the thin cantilever made of bronze. The bending rigidity of the cantilever was small in comparison with the longitudinal rigidity of the sample. As a result, the sample was subjected to the constant stress on the same way as the suspension wires of the antenna mirrors.

The signal on the detector output contains the spectral components corresponding to the oscillations of two different samples. A separation of the components was possible due

to the difference of its frequencies. It was based on the real time fast Fourier transform. The results of each experiment were the records of the amplitude and frequency for the two samples. Each value was a result of averaging over 0.2 sec ($180 - 380$ periods of oscillation for the frequencies $0.9 - 1.9$ kHz, typical for the stress values mentioned above). Hence, the effective bandwidth defined by 1024 points FFT was 5 Hz. The signal-to-noise ratio in this bandwidth was $10 \div 15$, witch allows to observe variations of the amplitude during the time interval shorter as compared to the relaxation time τ^* of the samples oscillations (typically $5 \div 12$ sec). The number of the tested samples was 8, the overall duration of observation was about 90 $hours$.

The analysis of the results consists of two different approaches. First was based on the amplitude averaging over the time interval $t = 3 \times \tau^*$. The obtained values A_t can be regarded as independent realizations of a stochastic process. The variation of these values is σ_{At}. This amplitudes has been compared with $\bar{A}$ in order to select statistically significant deviations. A χ^2 criterion has been used. Three different types of deviations has been observed:

i) The deviations cased by the stabilization system fault - covers less than 10% of all records, can be easily selected and rejected.

ii) Relatively short $(1 - 3\tau^*)$ rising of the amplitude to the $3 \div 4$ σ_{At} level happens up to 20 times per 10 hours of observation (see $table1$), that in some cases was a statistically significant exceedence of the Brownian motion amplitude.

iii) Relatively short (about 3 τ^*) rising of the amplitude over the 4 σ_{At} level happens twice just for one sample.

It is important, that the measured mean amplitude was always equal to the estimated value for the Brownian motion with the accuracy better than 15%. At the same time we have no reasonable explanation for the rising of the amplitude yet. Note, that the absence of any correlation between such events in the pairs of samples tested simultaneously confirms, from our point of view, an inner nature of such a behavior of the samples.

The second approach treated the variations of the oscillation amplitude during the time

short as compared to the relaxation time. The ems value of the variations is:

$$\Delta A_{ems} \simeq \sqrt{\frac{2kT}{m^*\omega^2}}\sqrt{\frac{2t}{3\tau^*}} \tag{3}$$

if the $\tau^* = 10\ sec$, $t = 0.2\ sec$ $\Delta A_{ems} \simeq 0.12\bar{A}$. The variations of amplitude are independent realizations of a stochastic process. The distribution of this process has to be close to Gaussian. The distributions obtained in experiments show excess quantity of the events than the variation of amplitude ΔA overcomes the $4 \times \Delta A_{ems}$ level (see *table*2). The number of such events varies from a few units to a few tens per 10 hours for the different samples. In many cases the number of the excessive events was statistically significant.

In additional the spectrum analysis of the amplitude records and crosscorrelation analysis of the records pairs have been done. No periodic excitations of the sample oscillation as well as pair correlation have been found. When the stress value exceeds the threshold value about 90% of breaking tension the slow decrease of the fundamental mode frequency was observed. It corresponds to the viscous flow of the steel. For example, for the sample 2 under the maximum stress (last column in the *tables*1, 2) the speed of flow was:

$$\frac{1}{L}\frac{\partial L}{\partial t} \simeq 6 \times 10^{-5}\ 1/hours \tag{4}$$

For the stress value below the threshold the speed of flow was less then the resolution limit of the method of measurement:

$$\frac{1}{L}\frac{\partial L}{\partial t} < 3 \times 10^{-6}\ 1/hours \tag{5}$$

II. DISCUSSION

The main conclusion from the results reported above is the existence of an excess noise in the fundamental violin mode oscillation of the well stressed steel wires. The intensity and magnitude of the spontaneous amplitude variations is substantially smaller than it was obtained earlier on the tungsten wires. Possible explanation is the more homogeneous inner grain-like structure of the steel in comparison with the bamboo-like structure of the tungsten.

The statistic of the noise varies significantly from sample to sample, which is an evidence of the nonuniform distribution of the noise sources within the samples. This variation was proved to be large enough to hide any dependence of the excess noise on the stress value. The presence of the excessive peaks even on the samples which did not evince viscous flow means that its origin differ from the mechanical shot noise. The fast variation of the oscillation amplitude could be a result of avalanche-like process within the small part of the sample, which originally contains some type of inhonogenety. As far as our method of research does not provide information about fine time and space structure of the noise, it is difficult to develop any detailed model.

Let us evaluate the magnitude of the possible rapid (during the time about 1 ms) test mass displacement induced by the excessive variations of the Brownian oscillation amplitude of the suspension wire observed in the experiments. If this variation happens during the time smaller as compared to the oscillation period, the magnitude of test mass displacement should be maximal:

$$\Delta X \simeq \frac{2g}{l\omega^2}\Delta x = 1 \times 10^{-15}\ cm \tag{6}$$

here $\Delta x = 4 \times 10^{-10}\ cm$ is an instant variation of the oscillations amplitude, $l = 20\ cm$ - suspension length, $\omega = 2\pi \times 2 \times 10^3\ Hz$ - fundamental mode frequency. It means that under certain conditions the excess noise in suspension wires could generate the kicks acted on the test masses and simulated the signal bursts.

Sample Number	1	2	2	3	2	2	2
Frequency, Hz (stress / breaking tension)	1441 (0.51)	1540 (0.59)	1647 (0.67)	1645 (0.67)	1749 (0.76)	1841 (0.84)	1955 (0.95)
time of observation, hours	9.25	3.52	2.69	3.34	5.06	2.33	9.25
Number of events when $A_t > (\overline{A} + 3\sigma_{At})$ [theory prediction]	17 [6]	7 [2]	6 [2]	5 [2]	7 [3.4]	3 [1]	18 [6]

Table 1.

The illustration of the excessive events

in the distribution of oscillation amplitude averaged over the interval

long as compared to the relaxation time.

Sample Number	1	2	2	3	2	2	2
Frequency, Hz (stress / breaking tension)	1441 (0.51)	1540 (0.59)	1647 (0.67)	1645 (0.67)	1749 (0.76)	1841 (0.84)	1955 (0.95)
time of observation, hours	9.25	3.52	2.69	3.34	5.06	2.33	9.25
Number of events when $\Delta A > 3\Delta A_{ems}$ [theory prediction]	865 [433]	162 [165]	155 [126]	257 [156]	249 [237]	134 [109]	546 [433]
Number of events when $\Delta A > 4\ \Delta A_{ems}$ [theory prediction]	115 [10]	2 [4]	5 [3]	8 [4]	7 [5]	16 [3]	40 [10]
Number of events when $\Delta A > 5\ \Delta A_{ems}$ [theory prediction]	7 [0]	0 [0]	0 [0]	0 [0]	2 [0]	6 [0]	4 [0]

Table 2.

The illustration of the excessive events

in the distribution of the amplitude variation averaged over the interval

short as compared to the relaxation time.

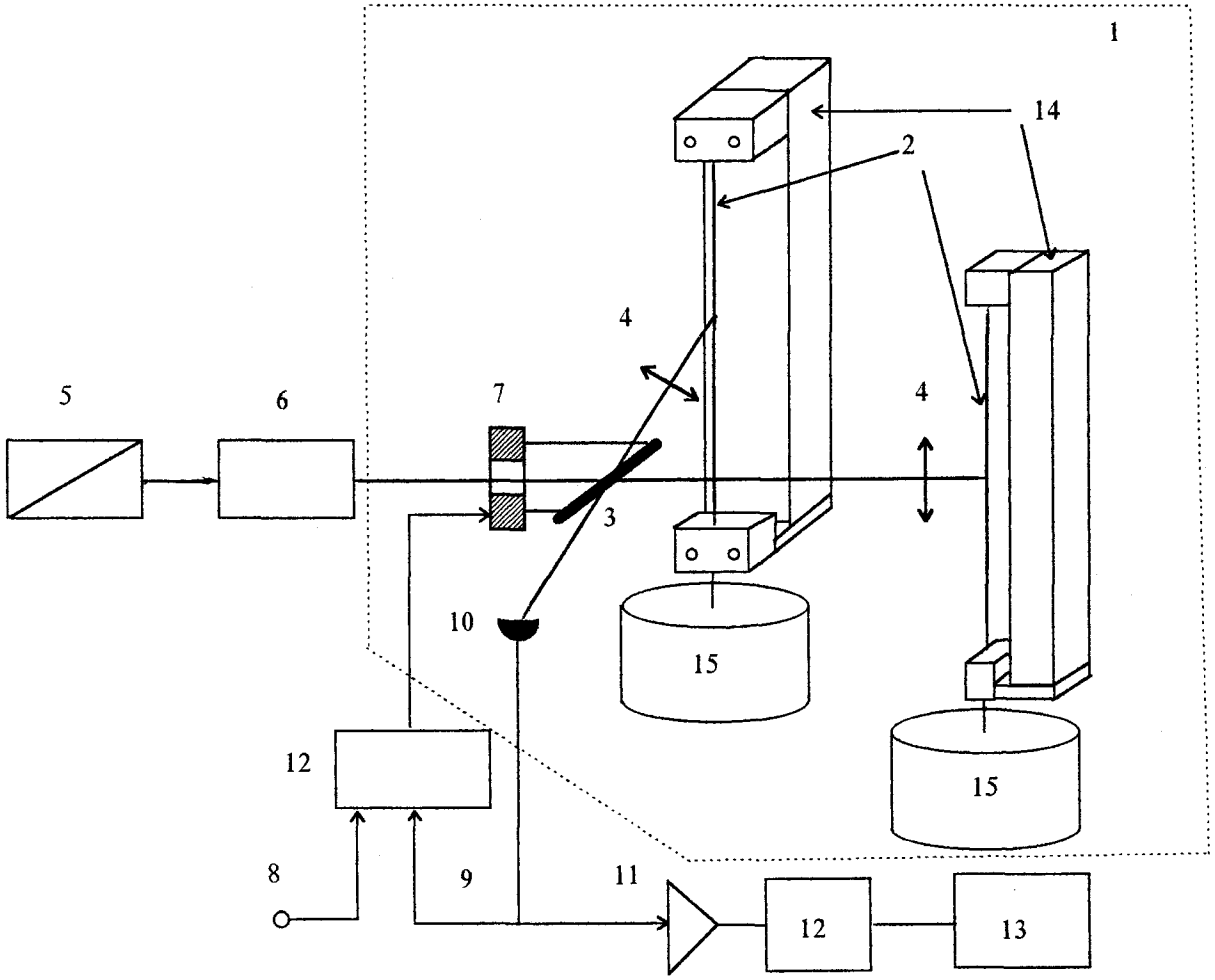

1. Vacuum chamber which contains fiber samples and readout interferometer.
2. Fiber sample.
3. PZT driven beam splitter.
4. Aspherical lens with a focal spot of 5 μm in diameter on fiber surface.
5. Helium-neon frequency-stabilised laser.
6. Optical insulator.
7. PZT drive.
8. Calibrating signal input.
9. Slow drift compensation loop.
10. Detector.
11. Low noise amplifier.
12. Band bass filter.
13. ADC.
14. Rigid frame for the fiber fixation.
15. Lead load.

Figure 1
Schematic diagram of the
interferometric readout for
the excess noise measurement

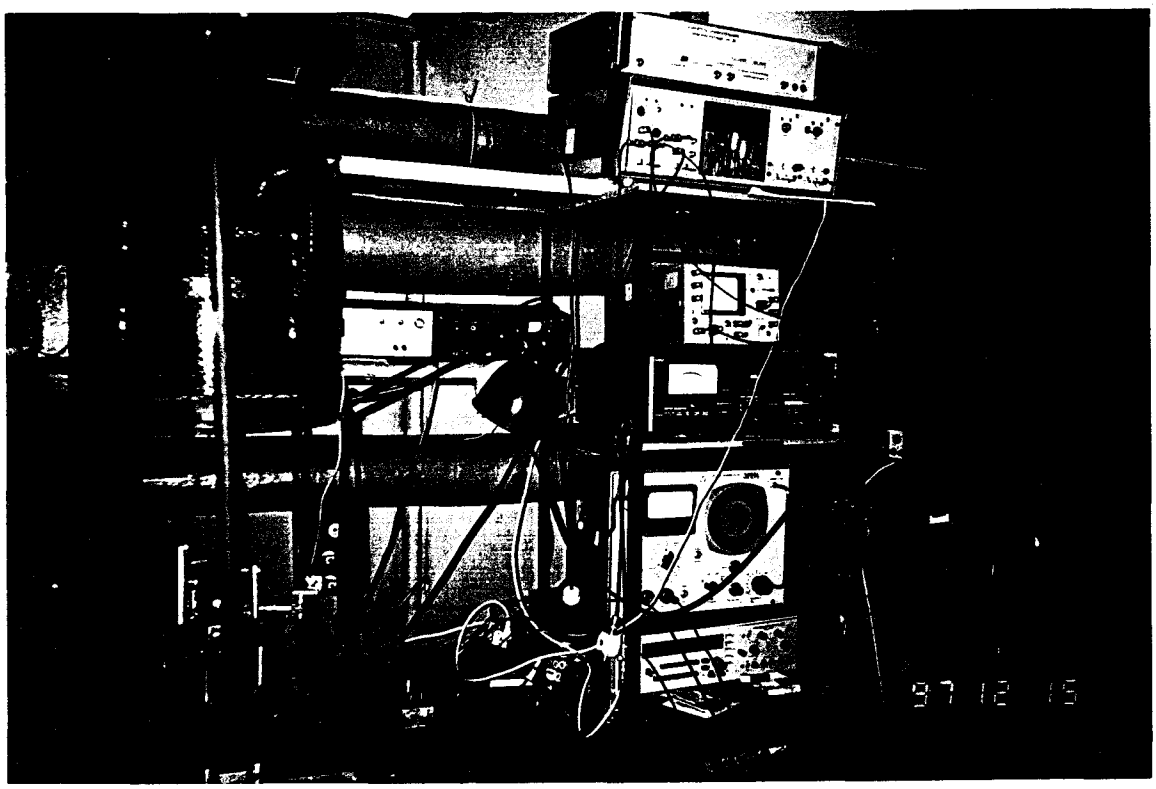

Figure 2

The picture of the vacuum chamber
and measurement devices

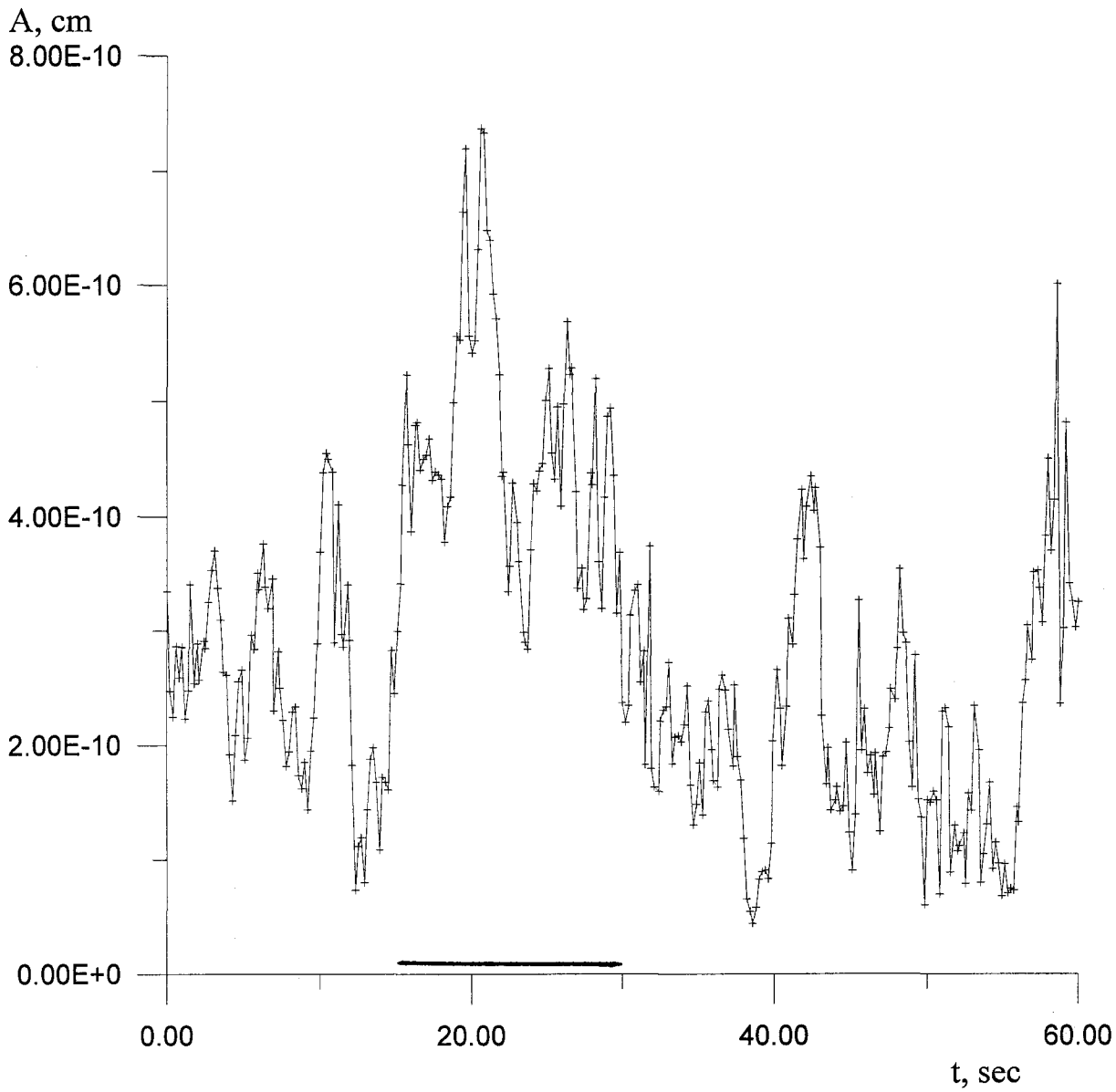

Figure 3

T ypical shape of the spontaneous rising
of the oscillations amplitude

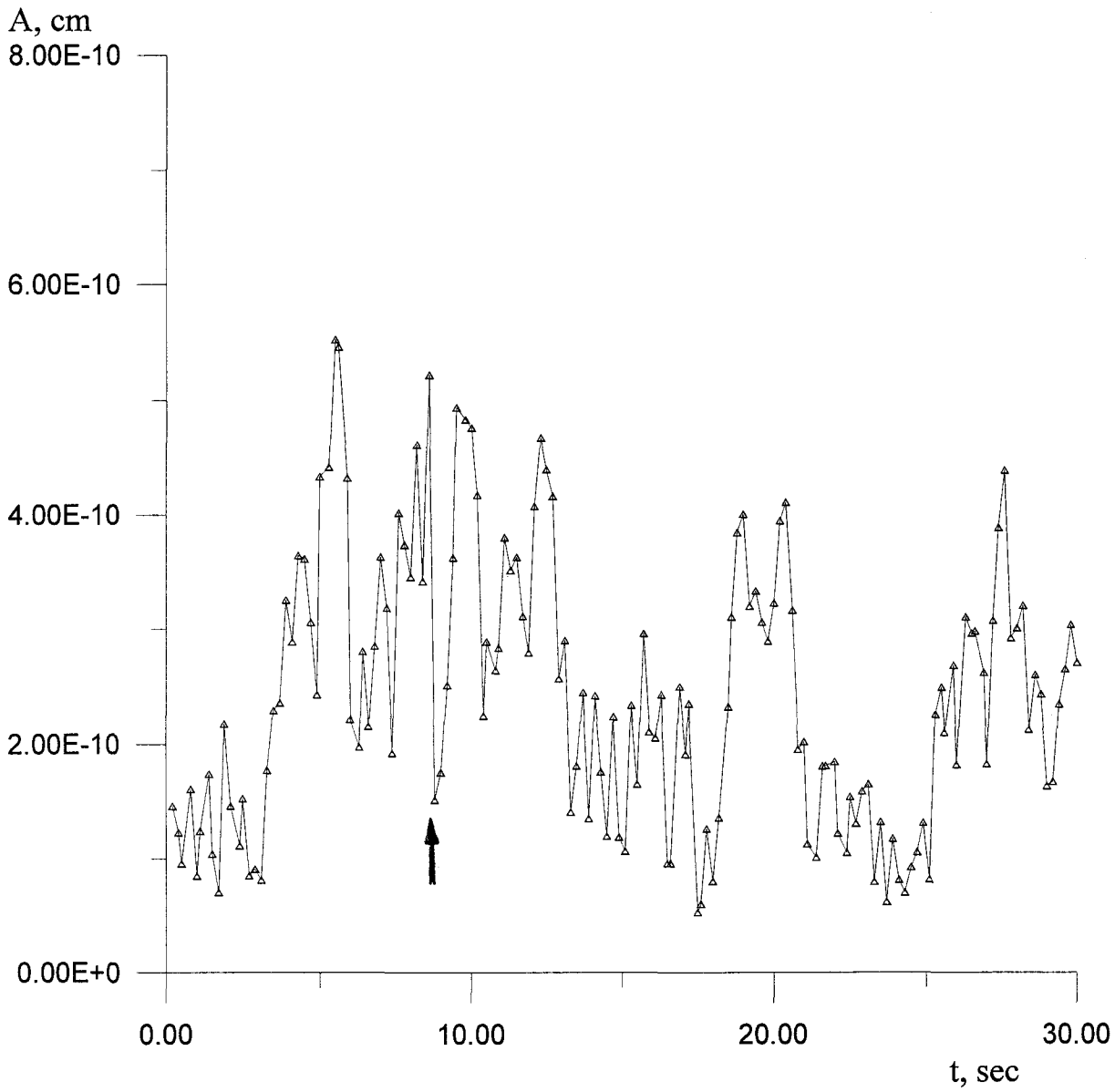

Figure 4

T. ypical time dependence of the amplitude
including one excessive variation event (spontaneous decreacing)

Appendix II

Design and development of a new vacuum chamber for tests of Q-factors in the suspension modes

One of the key goals of the MSU research group is to achieve the highest possible quality factors Q for the fused silica fiber suspensions' pendulum modes and violin modes with test masses near 2 kg. Record high Q - values for these modes about 1×10^8 have been demonstrated (see annual MSU group reports 1995 and 1996). This value is almost one order lower than can be expected from the reckons made on the base of the measured intrinsic losses in high-pure fused silica. But our attempts to increase Q were unsuccessful. Our research has shown that at the level of $Q = 10^8$ several dissipation mechanisms may make a contribution to the damping of the suspension pendulum mode in the experiments. We can point to the following. 1. The recoil losses caused by insufficient rigidity of the support for the pendulum. 2. Transfer of the energy to the molecules of the residual gas. 3. Surface losses in the fused silica suspension fibers in particular due to the sedimentation of silica vapours and dust particles on the fiber in the process of its fabrication. 4. The losses caused by the action of electric and magnetic fields in particular due to the electrostatic charges sitting on the fused silica test masses and on dielectric parts of the various equipment surrounding them.

In order to improve the quality-factors it is necessary to decrease substantially the influence of all these losses mechanisms. The experimental set-up which was used in previous (1996) our measurements does not permit to solve these problems. To achieve the maximum possible Q for the fused silica mass suspensions new chamber was developed, designed and tested. It is shown in Pictures 1a and 1b, the schematic design of the chamber is shown in Fig.2

The rigidity of the support structure for the pendulum was increased by attaching of a massive steel table of thickness 40 mm to the main wall of the laboratory building of thickness 1.5 m. This table was used for fastening of the top fused silica disk with the welded pendulum fiber and as a cover of the chamber. An estimated value of the equivalent rigidity K_{sup} for this support was approximately 10^{10} N/m. One can estimate the recoil losses for 2 kg pendulum (spring constant $K_{pen} \approx 10^2$ N/m) suspended from this support structure using a relationship: $Q^{-1}_{rec} = K_{pen}\, Q^{-1}_{sup} / K_{sup} \approx 10^{-9}$. Damping in the

support structure Q_{sup} is assumed to be approximately 10^{-1}. A value of the required vacuum in the chamber is determined by the residual gas damping Q_{gas}. According to our measurement of gas damping for pendulums to be tested the following relationship is valid: $Q_{gas} \approx (5\times10^{-3}) \times P(\text{Torr})$ for gas pressure $P < 3\times10^{-5}$ Torr. A vacuum level of approximately 3×10^{-8} Torr was achieved in the chamber after backing using a turbomolecular pump and an ion pump. Backing of the chamber and the pendulum at a temperature near 120°C is used to remove water from a surface of fused silica as well.

The system for excitation of the pendulum oscillation and the sensor for monitoring its motion as well as an arrester of the pendulum are designed in such a way that they were removed to sufficient distances from the pendulum. This permit to exclude the losses caused by electric fields from the accidental charges sitting on the surface of fused silica.

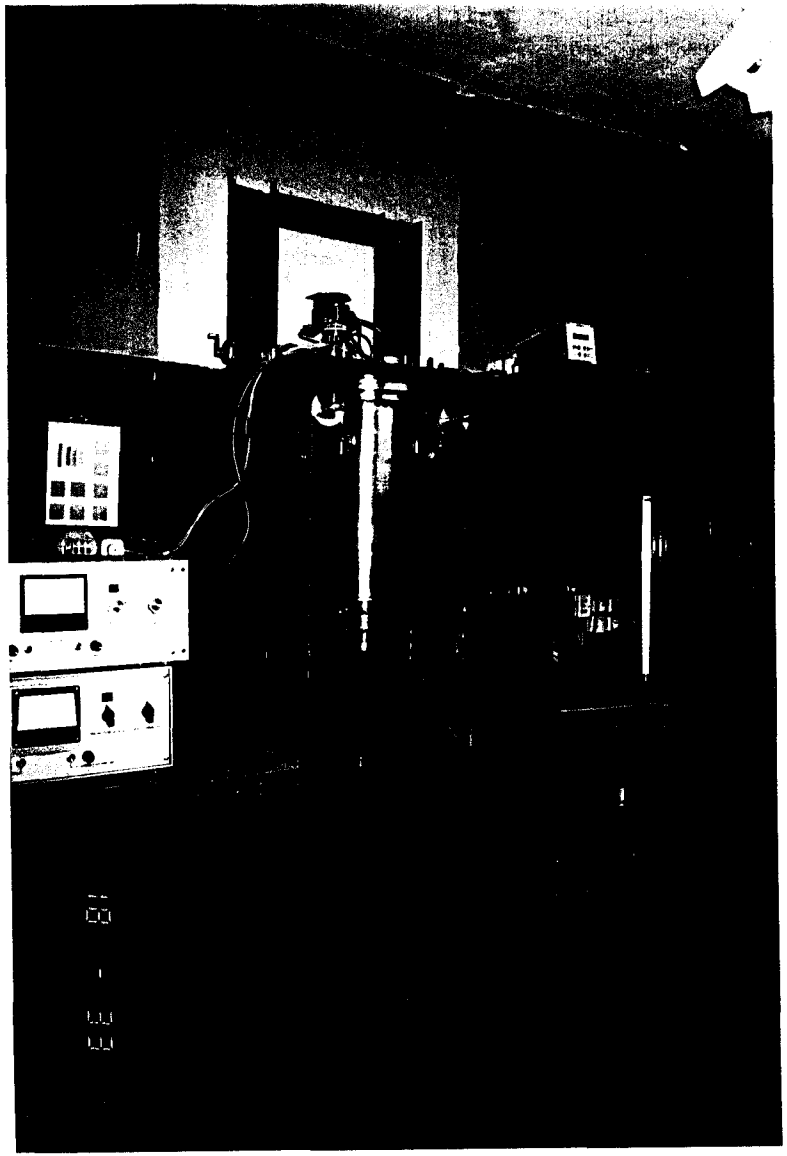

Picture 1a

Picture 1b

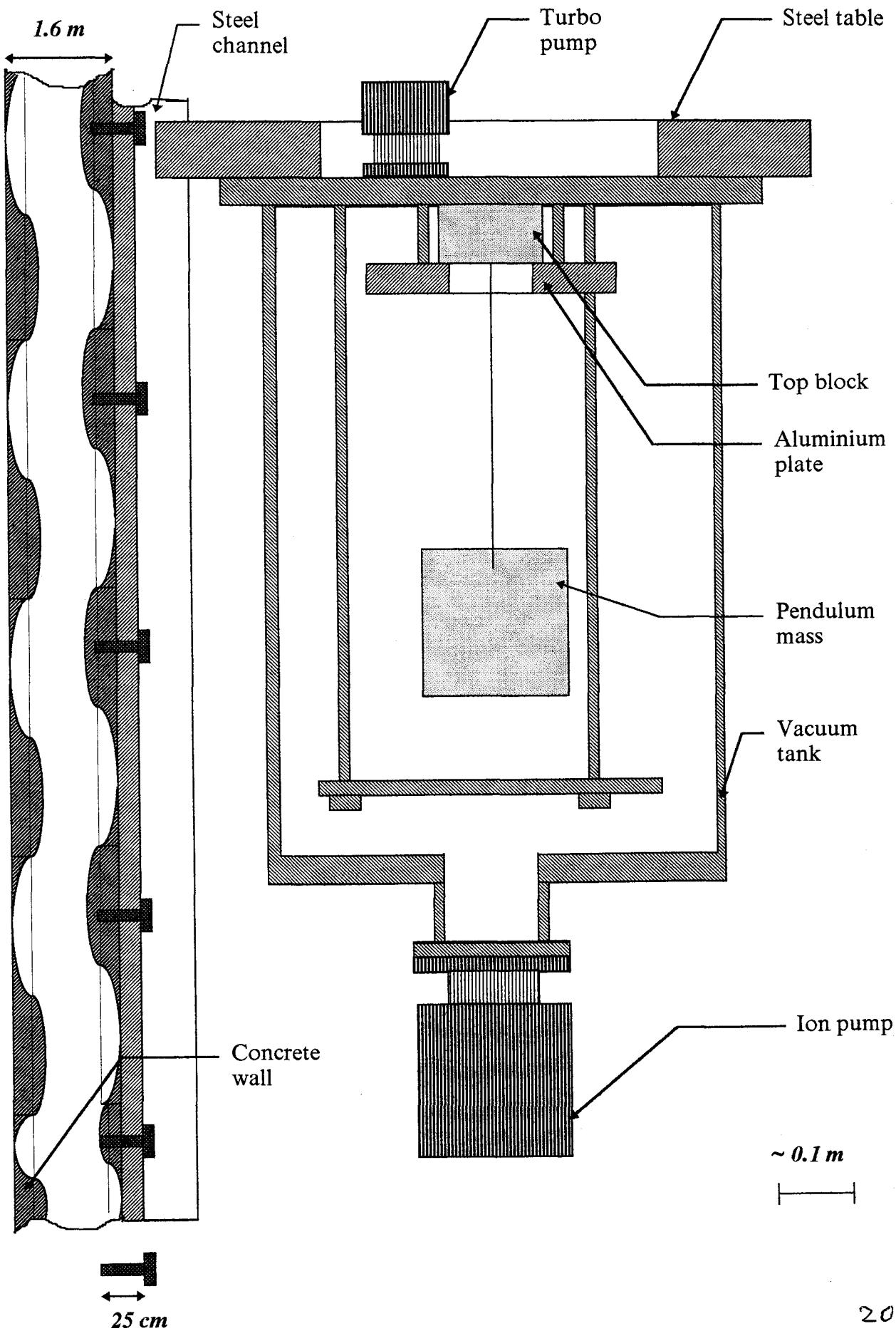
1.6 m
Steel channel
Turbo pump
Steel table
Top block
Aluminium plate
Pendulum mass
Vacuum tank
Ion pump
Concrete wall
~ 0.1 m
25 cm

Appendix III

The investigation of dynamical and dissipative actions of electric controller on the test mass

The electric controller will produce dynamical and dissipative actions on the test mass. In our previous preliminary experiments we observed the dissipative actions on the test mass due to the following processes: 1) the dissipative processes on the surface of conductors which are connected to the source of electric field; 2) electrostatic field produced by electric charges located on the surface of fused silica; 3) Joule losses in the resistive part of the controller's circuit. We describe below the results of our calculation and experimental investigations of dissipation introduced by electric controller into the test mass (the source #3). This damping is an inherent property of the electric driver system. It is not relevant to damping produced by the test mass servo control system and is not suppressed by the filter.

Consider a model of the electric controller shown schematically in Fig.1. The test mass m suspended as a pendulum is an oscillator with a spring constant $k = mg/l$. There is a capacitor plate of an area S separated by a small gap d from the conductive surface of the test mass. This plate is an electrode of the electric controller. The control voltage is applied to this electrode. In any case there is a resistor R in the circuit (an internal impedance of the voltage generator U). $C = \varepsilon_0 S / d$ is a capacitance between the electrode and the test mass. C_s is a stray capacitance which does not change in motion of the test mass.

In the general case the ac voltage $U = U_0 \cos pt$ can be used to produce the dc control force applied to the test mass due to a quadratic dependence of the force on the voltage. The advantage of ac voltage is an absence of dc electric field which may introduce a damping due to the dissipative electron processes on the surfaces.

Suppose that the change of the position of the test mass x is small in comparison with the gap $x/d << 1$. In this case the equation of motion for the test mass and for the charge q in the circuit are

$$m\ddot{x} + kx = -\frac{q^2\alpha^2\left[\, 1 - 2(1-\alpha)x / d_0) \,\right]}{C_0 d_0}, \qquad (1)$$

$$\dot{q}R + \frac{q}{C_0 + C_s}(1 + \alpha x / d_0) = U_0 \cos pt, \; . \qquad (2)$$

where $\alpha = C_0/(C_0+C_p)$, $d = d_0+x$.

When solving these equations we exclude any resonance and parametric action of the controller on the test mass by choosing the frequency $p \neq (m/l)\omega_0$ (here m and l are whole numbers, ω_0 is the resonance frequency of the oscillator). We also assume the amplitude of a constrained oscillation of the test mass with the frequency p to be much smaller then the amplitude of a free oscillation with the frequency ω_0 ,.

Finding the solution of the equations in the first approximation and calculating a ratio of the energy lost per period of oscillation to the stored energy we find the damping coefficient of the oscillator

$$Q^{-1} \approx \frac{U_0^2 R C_0^2}{2d_0^2 m\omega_0} \cdot \frac{1-(p^2-\omega_0^2)\tau^2}{(1+p^2\tau^2)\cdot\left[1+(p+\omega_0)^2\tau^2\right]\cdot\left[1+(p-\omega_0)^2\tau^2\right]}. \qquad (3)$$

Eq.(3) may be written in terms of the quasistatic displacement of the test mass Δx under the action of the force from the controller

$$Q^{-1} \approx \frac{2\Delta x\omega_0 R C_0}{d_0} \cdot \frac{\left[1-(p^2-\omega_0^2)\tau^2\right]}{\left[1+(p+\omega_0)^2\tau^2\right]\cdot\left[1+(p-\omega_0)^2\tau^2\right]}. \qquad (4)$$

Note that according to Eq. (4) with the constraint $(p^2-\omega_0^2)\tau^2 > 1$ the introduced damping becomes negative; that is, a regeneration of the oscillator is possible. This is the result of the additional delayed rigidity introduced in the oscillator by the controller.

The Johnson noise of the resistor R in the circuit of the controller is a source of the fluctuating force acting on the test mass. A calculation of the spectral density of this force gives

$$S_F(\Omega) = 4kTR\left(\frac{C_0U_0}{2d_0}\right)^2 \cdot \frac{\left[1+(p^2+\Omega^2)\tau\right]}{\left(1+p^2\tau^2\right)\cdot\left[1+(p+\Omega)^2\tau^2\right]\cdot\left[1+(p-\Omega)^2\tau^2\right]}. \qquad (5)$$

Comparing Eqs.(3) and (5) one can verify that the spectral density of the fluctuating force acting on the test mass is coupled with the introduced friction coefficient $H(\Omega)$, namely, the

sum of positive and modulus of negative parts according to the Fluctuation-dissipation theorem.

The experimental investigations of the damping introduced by the electric controller were carried out with the special pendulum. It was taken a reasonably large value of the resistor in the circuit of the electric controller R in order to obtain high damping and to exclude the influence of the other mechanisms of losses caused by electric field. The dependence of the introduced damping Q^{-1} on the value of the resistor R in the circuit of the electric controller in the case that dc voltage is applied is shown in Fig.2. In the case that ac voltage is applied the dependence of Q^{-1} on the frequency p of this voltage for R = *10GOhm* is shown in Fig.3. The experimental results are in a good agreement with the calculations to be carried out with a fitting parameter C_s. They are shown by the lines in Figs.2 and 3.

In the actual controller it is reasonable to choose the frequency $p \approx 10^6$ s^{-1} in order to decrease the amplitude of the constrained oscillation of the test mass. Substituting the parameters of the test mass and the electric controller to Eqs. (4) and (5) : m = 10 kg, ω_0 = 6 s^{-1} , S = 3 cm^2 , d = 10^{-1} cm, R = 10^3 Ohm, U = 250 V, one can obtain $Q^{-1} \approx 3\times10^{-12}$ and S_F $\approx 2\times10^{-30}$ N^2/Hz with the range of controller about 10^{-5} cm.

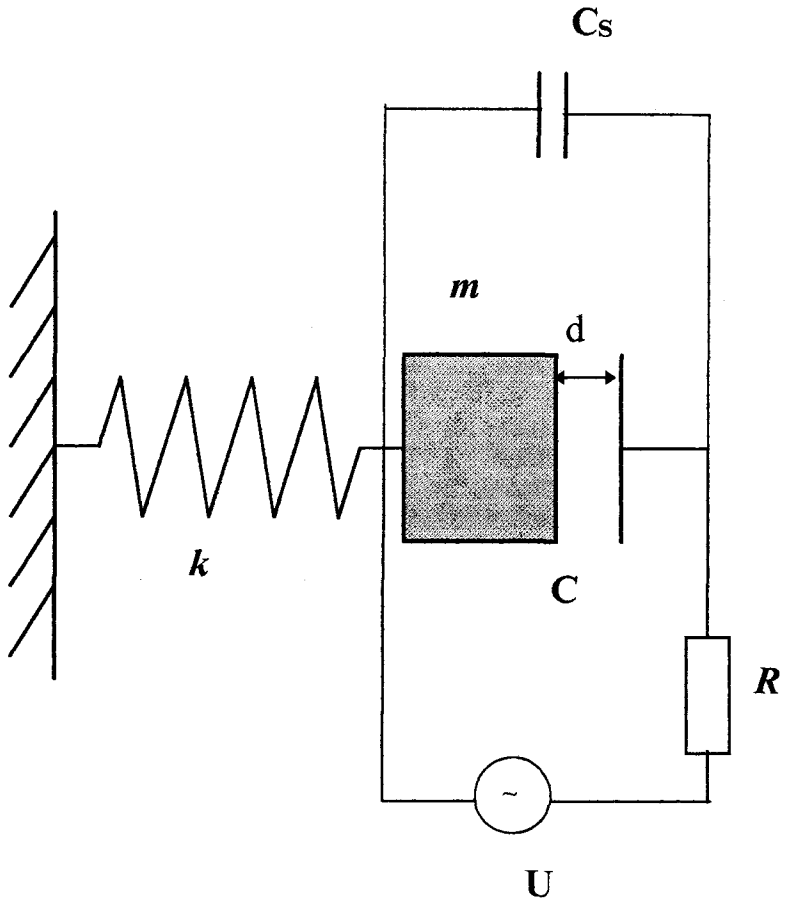

Fig.1

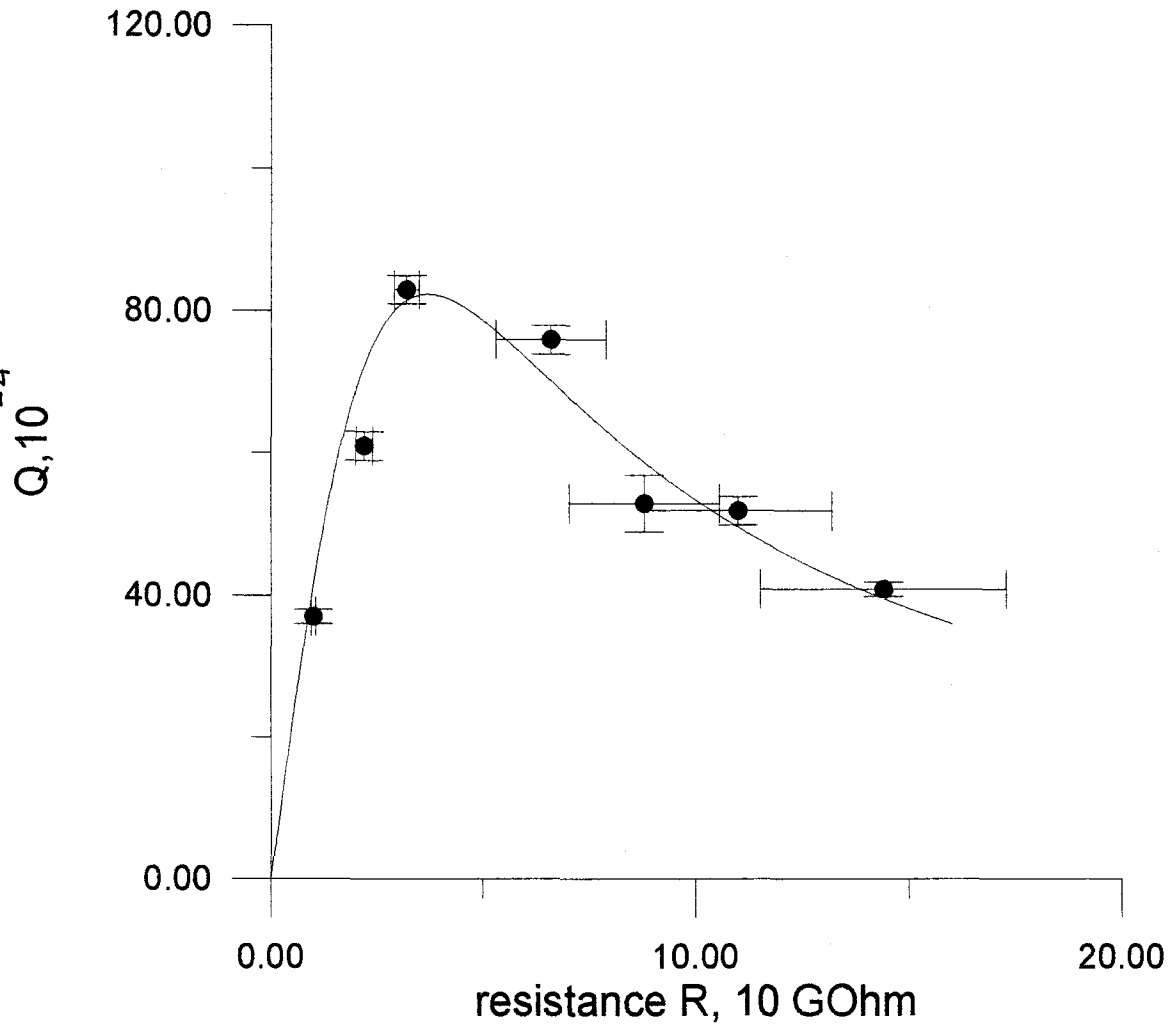

Fig.2

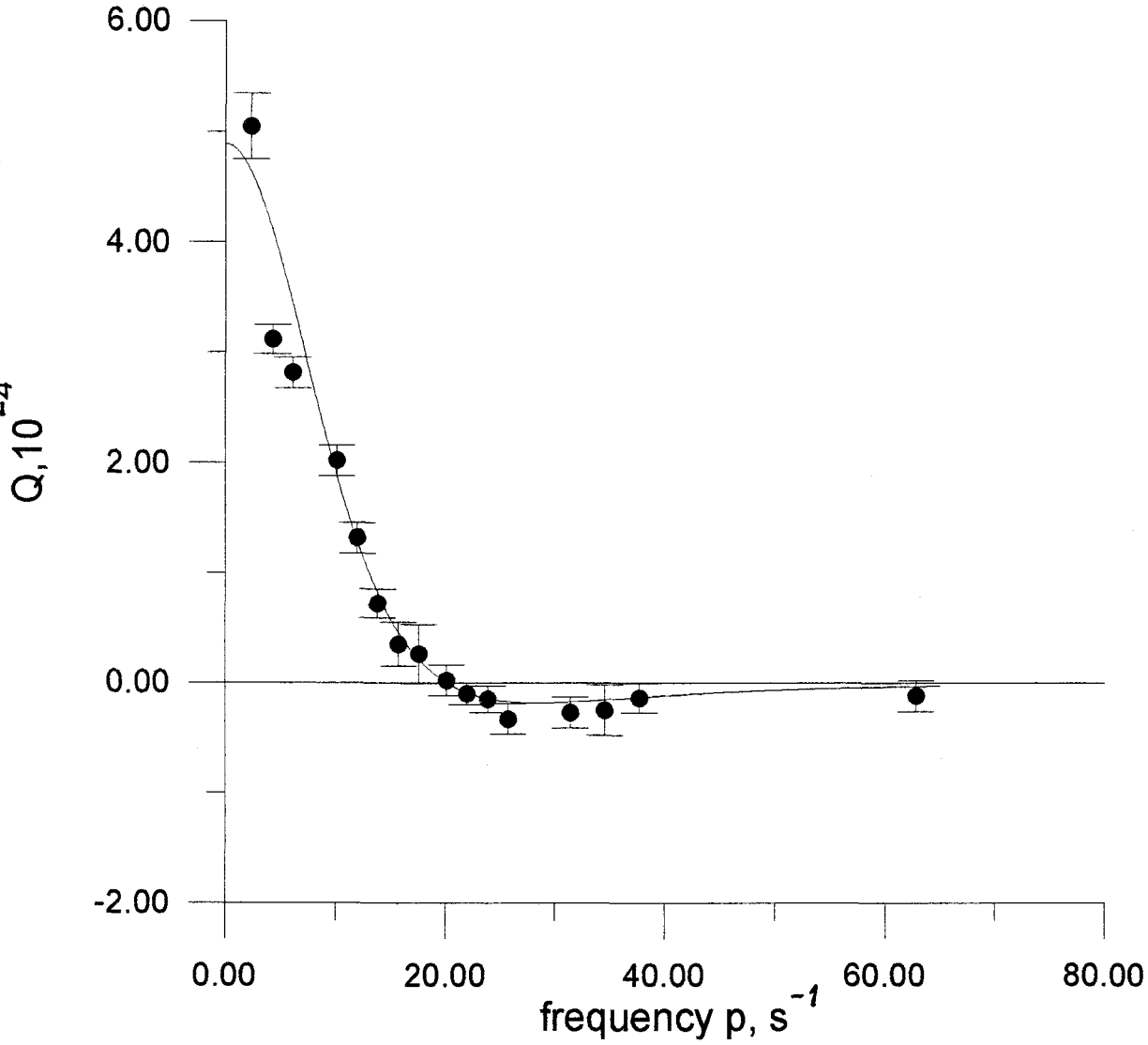
6.00
4.00
2.00
0.00
-2.00
Q,10^-4
0.00
20.00
40.00
60.00
80.00
frequency p, s^-1

Fig.3

Figure Captions

Fig.1 Schematic model of the electric controller.

Fig.2 Dependence of the introduced damping on a value of the resistor in the circuit of the electric controller for dc U = 1000 V.

Fig.3 Dependence of the introduced damping on a frequency of the applied voltage U= 360 V.

ELSEVIER

4 August 1997

PHYSICS LETTERS A

Physics Letters A 232 (1997) 340–348

Optical bars in gravitational wave antennas

V.B. Braginsky, M.L. Gorodetsky, F.Ya. Khalili

Department of Physics, Moscow State University, Moscow 119899, Russian Federation

Received 7 May 1997; accepted for publication 20 May 1997
Communicated by V.M. Agranovich

Abstract

A new scheme of gravitational wave antennas is proposed which due to the effect of light pressure behaves analogous to solid state antenna of the same scale. The gravitational signal in this scheme is transformed into the force acting on a mirror. The resulting mirror displacement may be detected using methods standard for the bar antennas. The scheme provides gain in resolution and allows one to beat the standard quantum limit without the use of non-classical pumping. © 1997 Published by Elsevier Science B.V.

1. Introduction

All known schemes of laser gravitational wave antennas, the first generation of which will be put into operation [1–4] in a few years, are based on the same principle. The gravitational signal is measured by a phase shift of the optical output wave. In such a case the main limiting factor is the quantum shot noise which leads to the necessity to increase pumping. In a previous paper [5] we proposed a new principle. Instead of extracavity measurement of the time phase shift it was suggested that the space phase shift be detected directly in the arms of a gravitational antenna using the principles of non-linear optics and quantum non-demolition measurements. A scheme was examined as an illustration in which the space phase shift produced by a gravitational wave converts to the phase shift in a microwave resonator coupled with thin transparent plates with cubic non-linearity, which are inserted in the optical system. At the same time for the planned parameters of laser gravitational wave antennas in the system there is a strong cubic non-linearity caused by the ponderomotive effect of the light pressure [6]. In this paper we analyze the possibility of using this "natural" non-linearity to transform the variation of the metric produced by the gravitational wave into the force acting on an additional mirror placed inside the optical resonator.

2. Energy redistribution in the system of the two coupled resonators

We start with examining two resonators of Fabry–Perot type with high finesse, having lengths $L_1 = L_2 = L$. Let these resonators be coupled, for example, by means of a mirror with a small transmittance coefficient T (see Fig. 1). Here we take absorption as negligible so that $R^2 + T^2 = 1$, where R is the reflectivity of the mirror. The influence of losses will be discussed in the next section.

Eigenfrequencies in such a system form a series of doublets. Frequencies in each doublet ω_+ and ω_- are apart from each other by (see Appendix A)

PII S0375-9601(97)00413-1

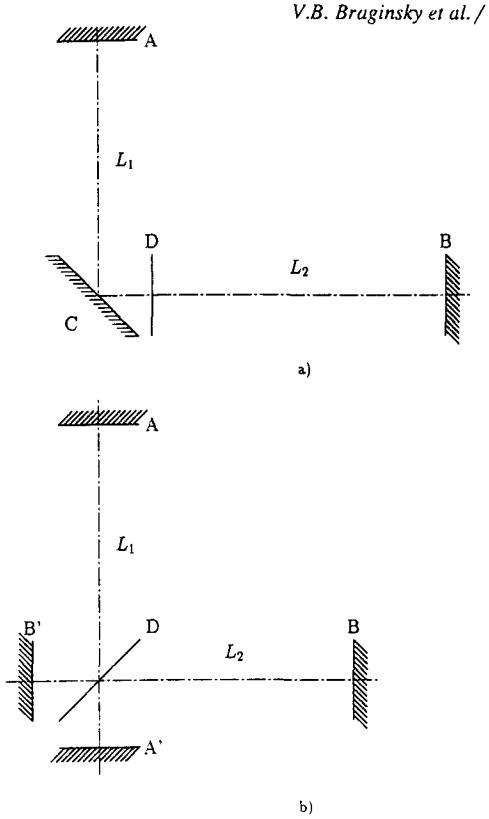

Fig. 1. Two topologies of antennas: (a) L-topology; (b) X-topology.

$$\Omega = \omega_+ - \omega_- = \frac{cT}{L},$$

where c is the speed of light. By choosing the appropriate transmittance T this value can be made to be close to the frequency of gravitational waves ω_{gr}.

Now we consider that by external pumping only one mode of the doublet, say ω_+, is excited. In this case the identical energy $\mathcal{E}/2$ will be stored in each Fabry–Perot resonator. A small change in the optical lengths of the resonators will result in an energy redistribution between the resonators, proportional to this change. In this paper we suggest that this effect be used for the detection of gravitational waves by measuring the difference of energies in the two coupled resonators. It is important that such a measurement must not be accompanied by the absorption of quanta, i.e. it is necessary to measure the energy difference in a QND way. One can suggest several variants of a concrete design for the realization of the given idea. The only condition needed is that partial frequencies in the two coupled resonators be changed differently under the action of gravitational waves. For example the L-scheme of the paper in Ref. [5] (Fig. 1a) or X-scheme, similar to that from Ref. [8] suggested for dual recycling (Fig. 1b). In both figures all mirrors except the coupling one, D, have in our approximation reflectivity equal to unity and the mirror D has a certain small coefficient of amplitude transmittance T. As calculations show, both schemes give similar results and so here, to be specific, we will analyze only the L-scheme.

As shown in Appendix B, the difference in optical energies in two arms of this new gravitational wave antenna $\delta\mathcal{E}(t)$ for an optimal orientation of the resonators and optimal polarization of the gravitational wave can be described by the following integral,

$$\delta\mathcal{E}(t) = \frac{\omega_0\mathcal{E}}{L}\int_{-\infty}^{t} \sin\Omega(t-t')\,\delta L(t')\,dt', \qquad (1)$$

where $\omega_0 = (\omega_+ + \omega_-)/2$ and $\delta L = Lh(t)$ is the difference in the resonators' lengths caused by the gravitational wave, $h(t)$ is the perturbation of the metric. This equality evidently is also valid if $L_1 \neq L_2$, but $|L_1 - L_2 - n\lambda/2| \ll T\lambda$, where n is an integer and λ is the optical wavelength. Formula (1) shows that the dynamics of the response to the external action is similar (without taking into account the constant factor) to those of the oscillator with frequency Ω. In particular, the response is maximal when the characteristic frequency of the gravitational wave $\omega_{gr} \simeq \Omega$.

Also may be of interest, at the same time, the quasistatic case, when the $h(t)$ signal slowly changes in comparison to the frequency Ω, as in this case the system is wideband – its coefficient of transformation weakly depends on the signal frequency. In this case,

$$\delta\mathcal{E}(t) = \mathcal{E}\frac{\omega_0\delta L(t)}{\Omega L}. \qquad (2)$$

For the measurement of relatively slow variations of $\delta\mathcal{E}(t)$ (with characteristic time $\simeq \omega_{gr}^{-1}$) one can use a non-linearity of ponderomotive origin. In other words, the most natural method of QND measurement of the value $\delta\mathcal{E}(t)$ will be the measurement of the difference force of optical pressure acting on the central coupling mirror D,

$$\delta F_p = -\frac{\delta\mathcal{E}(t)}{L}. \qquad (3)$$

This scheme is in essence similar to the principle of ponderomotive energy measurement [7].

In this case, the perturbation of the metric due to the gravitational wave in the suggested scheme is transformed into the displacement Δx_D of the mirror D caused by the force of the light pressure. This displacement is the absolute coordinate movement relative to an independent mass which is not in interaction with the optical wave. The optical field in this case behaves analogous to "horns" in the solid bar gravitational wave antennas [10], transforming a relative displacement of two butt-ends to the absolute movement of two close plates of the capacitance transducer. One can estimate the value of this effect. Substituting Eq. (2) into (3), we obtain $\delta F_p = (2\pi\mathcal{E}/T\lambda)h$, where $\lambda = 2\pi c/\omega_0$ is the optical wavelength. If $\mathcal{E} = 10^7$ erg, $\lambda = 10^{-4}$ cm, and $T = 10^{-2}$, then if $h = 3 \times 10^{-23}$, $\delta F_p \simeq 2 \times 10^{-9}$ din.

Evidently, the direct use of this relatively large value of δF_p for numerical estimates is incorrect, because in the analysis given above we have not taken into account the whole dynamics of this rather complex scheme caused by finite masses of all mirrors.

3. Dynamical behavior of the meter

When analyzing the dynamical properties of this measuring system it is sufficient to take into account only one doublet of the optical modes. Assuming that only processes with characteristic time $\tau \gg L/c$ are of interest, one can consider two coupled lumped oscillators instead of the distributed system. The equations of motion for the generalized coordinates q_1 and q_2 of the oscillators according to this model may be represented in the form

$$\ddot{q}_1 + \frac{\dot{q}_1}{\tau^*_{\rm opt}} + \omega_1^2(t)q_1 + \Omega\omega_0 q_2 = \frac{\omega_0}{\rho}[U_1^{\rm pump}(t) + U_1^{\rm fluct}(t)],$$

$$\ddot{q}_2 + \frac{\dot{q}_2}{\tau^*_{\rm opt}} + \omega_2^2(t)q_2 + \Omega\omega_0 q_1 = \frac{\omega_0}{\rho}[U_2^{\rm pump}(t) + U_2^{\rm fluct}(t)], \quad (4)$$

where $\tau^*_{\rm opt}$ is the energy relaxation time of the partial optical resonators, $U_{1,2}^{\rm fluct}$ and $U_{1,2}^{\rm pump}$ are, respectively, the fluctuational forces and pumping forces, ρ is the wave impedance, $\omega_{1,2}$ are the optical partial frequencies dependent on displacements of the mirrors $x_{A,B,D}$ and on the variation of metrics $h(t)$,

$$\omega_1(t) = \omega_0\left(1 - \frac{h(t)}{2} + \frac{x_A(t) - x_D(t)}{L}\right),$$

$$\omega_2(t) = \omega_0\left(1 + \frac{h(t)}{2} + \frac{x_D(t) - x_B(t)}{L}\right).$$

The whole self-consistent set of equations of motion of the system must also include equations for the mechanical degrees of freedom. We shall limit our consideration to the case when the mirrors are nearly free masses (the resonant frequencies of pendulums are much less than $\omega_{\rm gr}$), coupled with the external world only through a small mechanical dissipation. Mirror D is also connected with a meter of the mechanical coordinate. Let the relaxation time of the mechanical degrees of freedom be much longer than the time of measurement so one can ignore direct damping and consider only associated fluctuational forces $F_A^{\rm fluct}$, $F_B^{\rm fluct}$ and $F_D^{\rm fluct}$. Then the corresponding equations will be

$$M\ddot{x}_A = -\frac{\rho\omega_0}{L}q_1^2 + F_A^{\rm fluct}(t),$$

$$M\ddot{x}_B = \frac{\rho\omega_0}{L}q_2^2 + F_B^{\rm fluct}(t),$$

$$m\ddot{x}_D = \frac{\rho\omega_0}{L}(q_1^2 - q_2^2) + F^{\rm meter}(t) + F_D^{\rm fluct}(t), \quad (5)$$

where M is the mass of the mirrors A and B, m is that of D, $F^{\rm meter}$ is the fluctuational back-action of the coordinate meter on the mirror D.

Eqs. (4) and (5) form a complete set of equations describing the dynamics of the system. Its concrete behavior depends on the parameters of pumping. The choice of the pumping frequency is determined by requirements on the dynamical stability of the system. In Appendix D it is shown that in the case of pumping at a lower frequency of the doublet ω_- negative electromagnetic rigidity appears. For nearly free masses in the system it leads to asynchronous instability, which during a short time (of the order of Ω^{-1}) pushes the system out of the operational regime.

When pumping at the higher frequency of the doublet ω_+, the electromagnetic rigidity is positive. If

$$\mathcal{E} < \mathcal{E}_{\rm thres} = \frac{m^* L^2 \Omega^3}{8\omega_0}, \quad (6)$$

where $m^* = (1/m + 1/2M)^{-1}$ is the effective mass, then asynchronous instability is absent. For $L = 4$ km, $\Omega = 10^3$ s^{-1}, $T = 10^{-2}$, and $m^* = 10^3$ g, inequality (6) gives the threshold energy $\mathcal{E}_{\text{thres}} = 10^7$ erg. However, in this case there exists an oscillatory instability which rocks the system at frequency $\omega_{\text{inst}} \simeq \Omega$ with characteristic time $\tau_{\text{inst}} > \sqrt{\tau^*_{\text{opt}}/\Omega}$ (see Appendix C).

It is appropriate to introduce here the characteristic frequency Θ, caused by the optical rigidity, $\Theta^4 = 2\omega_0 \mathcal{E}\Omega/m^*L^2$. It is appropriate to note also that this analysis is valid only in the linear approximation when $x_{A,B,D} \ll \lambda T$ and when the energy at ω_+ is much larger than that at ω_-.

The described oscillatory instability is also inherent in narrowband recycling schemes. The asynchronous threshold instability must also be taken into account for standard schemes with recycling [8,9].

In gravitational antennas it is simple to achieve $\Omega\tau^*_{\text{opt}} \gg 1$. In this case, the condition $\Omega\tau_{\text{inst}} \gg 1$ is also satisfied, which makes it possible to inhibit the oscillatory instability, for example, by rare appropriate kicks at time intervals $\simeq \tau_{\text{inst}}$.

Eqs. (6) are solved in Appendices C, D. In the quasistatic case, $\omega_{\text{gr}} \ll \Theta \simeq \Omega/\sqrt{2}$, the signal displacement of the mass m is equal to (see formula (E.1) in Appendix D)

$$x_D^{\text{signal}}(t) = \frac{Lh(t)}{2}. \tag{7}$$

In this case the optical fields in the interferometer's arms work as rigid bars pushing mirror D.

If $\omega_{\text{gr}} \simeq \Theta \simeq \Omega/\sqrt{2}$ then the response $x_D^{\text{signal}}(t)$ has a resonance character (E.1). It means that the response of the mass m may substantially exceed the value of $Lh(t)/2$ if the gravitational burst is a long wave packet. In this case the optical bars behave like rigid springs.

4. Threshold sensitivity of the new antenna

It is convenient to present the results of the computation of the obtainable sensitivity in the described antenna in the form of several thresholds of detection, each dependent only on one source of dissipation or noise of the meter. As a reference characteristic value for comparison we will use the standard quantum limit (SQL) of the sensitivity, which in case of antennas with free masses is

$$h_{\text{SQL}} = \frac{\xi}{L\omega_{\text{gr}}}\sqrt{\frac{\hbar}{m^*\tau_{\text{gr}}}}, \tag{8}$$

where τ_{gr} is the duration of the gravitational wavepacket with a characteristic frequency ω_{gr}, ξ is a factor of the order of unity dependent on the form of the wavepacket. If $m^* = 10^3$ g, $\omega_{\text{gr}} = 600$ s^{-1} and $\tau_{\text{gr}} = 10^{-2}$ s (one period), $h_{\text{SQL}} \simeq 10^{-22}$.

4.1. Absorption in optical resonators

The absorption limited signal-to-noise ratio as it follows from formula (E.2) of Appendix E equals

$$\left(\frac{s}{n}\right)_{\text{opt.loss.}} = \frac{\Omega\tau^*_0\Theta^4L^2m^*}{2\hbar}\int_{-\infty}^{\infty}\frac{|h_\omega(\omega)|^2}{\Omega^2+\omega^2}\frac{\mathrm{d}\omega}{2\pi}, \tag{9}$$

where $h_\omega(\omega)$ is the spectrum of the metric variation $h(t)$. At optimal tuning, when $\omega_{\text{gr}} \simeq \Omega$ and $\Theta = \Omega$, one can deduce from formula (9) that the value of the minimal detectable signal is

$$h_{\text{opt.loss.}} = \frac{h_{\text{SQL}}}{\sqrt{\omega_{\text{gr}}\tau^*_{\text{opt}}}}. \tag{10}$$

Consequently, when $\omega_{\text{gr}}\tau^*_{\text{opt}} \geqslant 1$, which is easy to satisfy, the losses in the optical mirrors do not prevent one from obtaining a sensitivity better than that of the SQL.

4.2. Mechanical losses in the suspension of mirrors A and B

The SNR for mechanical fluctuations has a simple form,

$$\left(\frac{s}{n}\right)_{\text{mech.loss.}} = \frac{M^2L^2}{4\kappa T_M H_M}\int_{-\infty}^{\infty}\omega^4|h_\omega(\omega)|^2\frac{\mathrm{d}\omega}{2\pi},$$

where κ is Boltzmann constant, T_M is the temperature, H_M is the coefficient of friction. This value is equal to the SNR for the case of detection of the force $ML\ddot{h}(t)$ on a test mass $2M$. This limitation is inherent to all known methods of gravitational waves detection. Corresponding estimates which have been repeatedly cited

in the literature (see for example Ref. [11]) show that with the current experimental culture of the isolation of the test masses, crossing the SQL becomes possible.

4.3. Noise terms of coordinate meter and of suspension losses of mirror D

It is known that the output signal of a meter of coordinate $x(t)$ may be represented in the form [12] $\tilde{x}(t) = x(t) + x^{\text{meter}}(t)$, where $x^{\text{meter}}(t)$ is the additive noise of the meter. The ultimate sensitivity of the detection system essentially depends on the character of the autocorrelation functions of noise terms $F^{\text{meter}}(t)$ and $x^{\text{meter}}(t)$ and on their crosscorrelation. Up to now several methods have been suggested, allowing one to overcome the standard quantum limit by choosing parameters of these noise terms, staying in the domain of the coordinate measurement. These methods may also be used in our scheme. However, their analysis lies outside the framework of this paper, so here we will limit ourselves with only an analysis of the simplest case of uncorrelated white noise terms of the meter $x^{\text{meter}}(t)$ and $F^{\text{meter}}(t)$. In this case the signal-to-noise ratio on the background of noise terms of the meter and noise $F_D^{\text{fluct}}(t)$, caused by mechanical losses in suspension of the mirror D, has the form

$$\left(\frac{S}{n}\right)_{\text{meter}} = \frac{M^2\Theta^8L^2}{(2M+m)^2}\int_{-\infty}^{\infty}\omega^4|h_\omega(\omega)|^2 \times\left[\frac{1}{\omega^4}(\omega^4-\omega^2\Omega^2+\Theta^4)^2S_x + \left(\omega^4-\omega^2\Omega^2+\frac{m\Theta^4}{2M+m}\right)^2\frac{S_F+S_m}{m^2}\right]^{-1}\frac{d\omega}{2\pi}, \tag{11}$$

where S_x and S_F are the spectral densities of the noise terms $x^{\text{meter}}(t)$ and $F^{\text{meter}}(t)$, which must correspond to the uncertainty relation [12]

$$S_xS_F \geqslant \frac{\hbar^2}{4},$$

and

$$S_m = \frac{2\kappa T_m m}{\tau_m^*}$$

is the spectral density of the noise $F_D(t)$, τ_m^* is the mechanical relaxation time for the mass m.

Formula (11) has a rather bulky appearance. In the dependence on the signal spectrum and values of parameters of the system different limits of sensitivity are possible. We consider two characteristic special cases.

Quasistatic case. Let condition $\omega_{\text{gr}} \ll \Omega \simeq \Theta$ be satisfied. In this case

$$\left(\frac{S}{n}\right)_{\text{meter}} = M^2L^2\int_{-\infty}^{\infty}\frac{\omega^4|h_\omega(\omega)|^2}{(2M+m)^2\omega^4S_x+S_F+S_m}\frac{d\omega}{2\pi}.$$

If the average value of the signal equals zero as in the case of gravitational waves detection, and dissipation is small enough,

$$\frac{2\kappa T_m\tau_{\text{gr}}^2}{\tau_m^*} < \hbar, \tag{12}$$

then the value of the minimal detectable amplitude of the metric variation will be equal to

$$h \simeq \sqrt{1+\frac{m}{2M}}\,h_{\text{SQL}},$$

i.e. for $m < M$ it corresponds to SQL. For the parameters given above, inequality (12) at room temperature gives $\tau_m^* > 8\times10^9$ s, which looks possible in the near future [11,13].

Resonant case. If the spectrum of the signal is concentrated near frequency $\omega_{\text{gr}} = \Omega/\sqrt{2}$, then the resonant character of the expression under the integral in formula (11) allows one to obtain a sensitivity better than the SQL. The price will be a longer time of detection $\tau_{\text{meas}} \gg \tau_{\text{gr}}$, and as a consequence a more serious requirement on dissipation for the following inequality to be fulfilled,

$$\frac{2\kappa T_m\tau_{\text{meas}}^2}{\tau_m^*} < \hbar. \tag{13}$$

Let us assume that $\Theta = \omega_{\text{gr}}$, which corresponds to the maximal permitted energy $\mathcal{E}$. In this case it follows from expression (11), that

$$h \simeq \frac{h_{\text{SQL}}}{\omega_{\text{gr}}\sqrt{\tau_{\text{gr}}\tau_{\text{meas}}}}. \tag{14}$$

Consequently, by increasing τ_{meas} up to the limit set by expression (13) or by cooling the test mass, it is possible to obtain a sensitivity better than the standard quantum limit.

5. Conclusion

Summing up the above discussion of the new scheme of laser gravitational wave antenna with a ponderomotive parametric amplification of the response, it is appropriate to emphasize the following specific features of the scheme.

(1) At an optimal value of the optical energy $\mathcal{E}$ in both arms of the resonator (see formula (7)) a burst of gravitational radiation with amplitude h leads to a force action on the central mirror D and produces, in the case of a wideband signal, its oscillations with amplitude Δx_D equal to $hL/2$. In the case of a narrowband signal, resonant amplification of the response is possible. In this way, the gravitational wave antenna has all the advantages of the solid state bar antenna with the characteristic dimensions of a laser one (4 km for the LIGO project). If $m = 10^3$ g, then, for $\omega_{gr} = 10^3$ s^{-1}, the optimal value $\mathcal{E} \leqslant 10^7$ erg. If $\tau^*_{opt} = 10$ s (corresponding to the value of the mirrors' finesse available today) then the required pumping power is only $W \simeq 10^6$ erg/s. For the detection of weak oscillations of the central mirror relative to the additional test mass interacting with the optical field one may use any detector developed for bar antennas, for example, a microwave parametric transducer [14]. In this case the following condition must be satisfied,

$$\Delta x_D \simeq \frac{hL}{2} \geqslant \frac{\alpha d}{\omega_{mw}\tau_{meas}\sqrt{N_{mw}}},$$

where

$$d = \omega_{mw}\left(\frac{d\omega_{mw}}{dx}\right)^{-1}$$

is the parameter of tunability of a microwave resonator, ω_{mw} is the microwave frequency, τ_{meas} is the duration of the measurement, N_{mw} is the number of used microwave quanta and α is the noise factor of the microwave amplifier. The value nowadays achieved for the factor $\alpha d/\omega_{mw}\tau_{meas}$ is $\simeq 3 \times 10^{-9}$ cm [14]. As a result the required microwave power is also not too large: if $h = h_{SQL} \simeq 10^{-22}$, then $W_{mw} \simeq 10^3$ erg/s.

For interferometric measurement in laser gravitational antenna, the response (time phase shift of the output wave) equals

$$\Delta\phi \simeq Kh\omega_o\tau_{gr},$$

where K is a dimensionless parameter equal to unity for optimal tuning. In the scheme examined in this paper, the factor

$$K = \frac{L\omega_{mw}}{d\omega_o} \simeq 10^4.$$

In other words, the scheme described provides essential amplification of the response.

(2) The sensitivity of our scheme is not limited by the standard quantum limit if $\omega_{gr}\tau_{meas} \gg 1$ (see formula (14)). Moreover, in the coordinate meter one can use any of the non-stationary schemes of measurement suggested before [15], allowing us to beat the SQL. The origin of this key advantage is that the fluctuations in the optical part of the meter may be in principle totally excluded and the only source of back-action will be the meter, which in case of the microwave transducer consumes very small energy.

(3) It is reasonable to note that the ultimate sensitivity and the optical pump power needed in this scheme do not depend on the quantum state of the pump field. The required state of the e.m. field in the resonator with a well-determined energy difference in the two arms of the antenna forms automatically in the process of monitoring the coordinate of the coupling mirror.

Acknowledgement

This paper was supported in part by the National Science Foundation, USA, (grant No. PHY-9503642), the California Institute of Technology and by the Russian Foundation of Fundamental Research.

Appendix A. The eigenfrequencies of the resonator

Let $a_{1,2}$ be the traveling waves' amplitudes running from mirror D (see Fig. 1a), $L_{1,2}$ are the lengths of the left and right arms. If A and B are absolutely reflective mirrors then the boundary conditions for the mirror D yield

$$a_1 = Ra_1 e^{2ikL_1} - iTa_2 e^{2ikL_2},$$

$$a_2 = Ra_2 e^{2ikL_2} - iTa_1 e^{2ikL_1},$$

where $k = \omega_0/c$ is the wavenumber. The characteristic equation for this system of equations has the form

$$\cos 2kL - R\cos k(L_1 - L_2) = 0.$$

If $k(L_1 - L_2) \ll 1$ and $T = \sqrt{1-R^2} \ll 1$, we obtain

$$\omega_{opt} \simeq \frac{n\pi c}{L} \pm \frac{\Omega}{2},$$

$$\Omega = \frac{c}{L}\arcsin T \simeq \frac{cT}{L}.$$

where n is an integer. In the case of the X-scheme (Fig. 1b) the characteristic equation gives $\Omega \simeq 2cT/L$.

Appendix B. The redistribution of the energy

Let us consider a pair of coupled resonators with slowly varying partial frequencies,

$$\omega_{1,2}(t) = \omega_0\left(1 \mp \frac{h(t)}{2}\right).$$

The equations of motion for this system have the form

$$\ddot{q}_1(t) + \omega_1^2(t)q_1(t) + \Omega\omega_0 q_2(t) = 0,$$
$$\ddot{q}_2(t) + \omega_2^2(t)q_2(t) + \Omega\omega_0 q_1(t) = 0, \qquad \text{(B.1)}$$

where $q_{1,2}$ are the coordinates of the oscillators.

Eqs. (B.1) can be transformed to the equations for the normal coordinates $q_\pm(t) = (q_1(t) \pm q_2(t))/\sqrt{2}$:

$$\ddot{q}_+(t) + \omega_+^2 q_+(t) = \omega_0^2 h(t) q_-(t),$$
$$\ddot{q}_-(t) + \omega_-^2 q_-(t) = \omega_0^2 h(t) q_+(t),$$

where $\omega_\pm = \omega_0 \pm \Omega/2$ are the eigenfrequencies (terms of the order higher than linear are neglected).

Let initially the mode with the higher eigenfrequency ω_+ only be excited:

$$q_+(t) = q_0 \cos\omega_+ t.$$

In this case,

$$q_-(t) = \omega_0 q_0 \int_{-\infty}^{t} \sin\omega_-(t-t')\cos\omega_+ t' h(t')\,dt'.$$

Hence the normalized difference of the energies of the partial oscillators is equal to

$$\frac{\delta\mathcal{E}(t)}{\mathcal{E}} = \frac{q_2^2(t) - q_1^2(t)}{q_2^2(t) + q_1^2(t)} = \frac{2q_+(t)q_-(t)}{q_+^2(t) + q_-^2(t)}$$
$$= \omega_0 \int_{-\infty}^{t} \sin\Omega(t-t')h(t')\,dt',$$

where $\mathcal{E}$ is the total energy in the system.

Appendix C. The dynamics of the system

Eqs. (4), (5) yield the full set of the equations of motion of the system,

$$\ddot{q}_+(t) + 2\delta_{opt}\dot{q}_+(t) + \left(\omega_+^2 + \omega_0^2\frac{\sqrt{2}x_-(t)}{L}\right)q_+(t)$$
$$+ 2\omega_0^2\left(\frac{x_+(t)}{\sqrt{2}L} - \frac{x_D(t)}{L} - \frac{h(t)}{2}\right)q_-(t)$$
$$= \frac{\omega_0}{\rho}[U_+^{pump}(t) + U_+^{fluct}(t)],$$

$$\ddot{q}_-(t) + 2\delta_{opt}\dot{q}_-(t) + \left(\omega_-^2 + \omega_0^2\frac{\sqrt{2}x_-(t)}{L}\right)q_-(t)$$
$$+ 2\omega_0^2\left(\frac{x_+(t)}{\sqrt{2}L} - \frac{x_D(t)}{L} - \frac{h(t)}{2}\right)q_+(t)$$
$$= \frac{\omega_0}{\rho}[U_-^{pump}(t) + U_-^{fluct}(t)],$$

$$M\ddot{x}_+(t) = -\frac{\sqrt{2}\rho\omega_0}{L}q_+(t)q_-(t) + F_+^{fluct}(t),$$

$$M\ddot{x}_-(t) = -\frac{\rho\omega_0}{\sqrt{2}L}[q_+^2(t) + q_-^2(t)] + F_-^{fluct}(t),$$

$$m\ddot{x}_D(t) = \frac{2\rho\omega_0}{L}q_+(t)q_-(t) + F^{meter}(t) + F_D^{fluct}(t), \qquad \text{(C.1)}$$

where $U_\pm^{pump}(t)$ are the pumps, $\delta_{opt} = 1/2\tau^*$, $U_\pm^{fluct} = (U_1^{fluct} \pm U_2^{fluct})/\sqrt{2}$, $x_\pm = (x_A \pm x_B)/\sqrt{2}$, $F_\pm^{fluct} = (F_A^{fluct} \pm F_B^{fluct})/\sqrt{2}$.

Let only one mode with frequency either ω_+ (down-conversion regime) or ω_- (up-conversion regime) be pumped, $U_\pm^{pump}(t) = U_0\sin(\omega_\pm t)$, $U_\mp(t) = 0$. Linearizing Eqs. (C.1) in the approximation of strong

pumping and using the method of slowly varying-amplitudes, one obtains

$$\dot{a}(t) + \delta_{\rm opt} a(t) \pm \Omega b(t) = -\frac{U_s^{\rm fluct}(t)}{\rho},$$

$$\dot{b}(t) + \delta_{\rm opt} b(t) \mp \Omega a(t) = \omega_0 q_0 \left(\frac{h(t)}{2} - \frac{x_+(t)}{\sqrt{2}L} + \frac{x_D(t)}{L} \right) + \frac{U_c^{\rm fluct}(t)}{\rho},$$

$$M\ddot{x}_+(t) = -\frac{\rho\omega_0 q_0}{\sqrt{2}L} a(t) + F_+^{\rm fluct}(t),$$

$$m\ddot{x}_D(t) = \frac{2\rho\omega_0 q_0}{L} a(t) + F^{\rm meter}(t) + F_D^{\rm fluct}(t), \qquad \text{(C.2)}$$

where q_0 is the mean amplitude of the pumped mode, $a(t)$ and $b(t)$ are the slowly varying-amplitudes of the other mode, and $U_{c,s}^{\rm fluct}(t)$ are the fluctuational sine and cosine components of the $U_{\mp}^{\rm fluct}(t)$.

The characteristic equation for the system (C.2) is the following,

$$p^2[p^4 + 2\delta_{\rm opt} p^3 + (\delta_{\rm opt}^2 + \Omega^2)p^2 \pm \Theta^4] = 0. \qquad \text{(C.3)}$$

Appendix D. On the dynamics stability

D.1. Down-conversion regime

The roots of the characteristic Eq. (C.3) in this case may easily be found in the approximation of small $\delta_{\rm opt}$. If $\delta_{\rm opt} = 0$, then

$$p_0 = \pm\sqrt{-\frac{\Omega^2}{2} \pm \sqrt{\frac{\Omega^4}{4} - \Theta^4}}$$

(both $\pm$ signs are independent, and we do not consider the trivial root $p = 0$). If $\Theta^4 < \Omega^4/4$ then all roots are purely imaginary and the system is stable.

For small $\delta_{\rm opt} \neq 0$ the roots may be presented in the form $p = p_0 + p'$, where p' is a small variance in the linear approximation proportional to $\delta_{\rm opt}$. If $\Theta \ll \Omega$ then

$$p' \simeq \frac{\delta_{\rm opt} p_0^2}{2p_0^2 + \Omega^2}.$$

If $\Theta \to \Omega/\sqrt{2}$ then

$$p' \simeq \frac{\pm 1 \pm i}{\sqrt{2}} \sqrt{\frac{\delta_{\rm opt}\Omega}{\sqrt{2}}}.$$

Some roots have positive real parts which, however, are small in comparison with the roots' absolute values. This corresponds to relatively weak oscillatory instability.

D.2. Up-conversion regime

For $\delta_{\rm opt} = 0$ the roots of the characteristic equation (C.3) are equal to

$$p_0 = \pm\sqrt{-\frac{\Omega^2}{2} \pm \sqrt{\frac{\Omega^4}{4} + \Theta^4}}.$$

One of these roots has a large positive real part. In this way the system is strongly asynchronously unstable. This result may be proved more rigorously and generalized on the case of $\delta_{\rm opt} \neq 0$ by using the Raus–Gurvitz criterion. This shows that the system is unstable if pumped at a lower frequency for all parameter values.

Appendix E. Signal-to-noise ratio

Using the spectral representation one can obtain from the set of equations (C.2) that the spectrum of $x_D(t)$ is equal to

$$x_{D\omega}(\omega) = x_\omega^{\rm signal}(\omega) + X_\omega(\omega),$$

where

$$x_\omega^{\rm signal}(\omega) = \frac{M\Theta^4 L}{2M + m} \times \frac{-\omega^2 h_\omega(\omega)}{\mathrm{Det}(\omega)} \qquad \text{(E.1)}$$

is the spectrum of the signal,

$$X_\omega(\omega) = \frac{1}{\mathrm{Det}(\omega)} \times \left[\left(-\omega^2[(i\omega + \delta_{\rm opt})^2 + \Omega^2] + \frac{m\Theta^4}{2M + m} \right) \times \frac{F_\omega^{\rm meter}(\omega) + F_{D\omega}^{\rm fluct}(\omega)}{m} + \frac{\sqrt{2}\Theta^4}{2M + m} F_{+\omega}^{\rm fluct}(\omega) + \frac{\omega_0 q_0 \omega^2}{mL} \times [\Omega U_{c\omega}^{\rm fluct}(\omega) + (i\omega + \delta_{\rm opt}) U_{s\omega}^{\rm fluct}(\omega)] \right],$$

is the spectrum of fluctuations of $x_D(t)$, $F_\omega^{\text{meter}}(\omega)$ is the spectrum of $F^{\text{meter}}(t)$ and so on, and

$$\text{Det}(\omega) = \omega^2[\omega^2(\Omega^2 - \omega^2 + 2i\delta_{\text{opt}}\omega + \delta_{\text{opt}}^2) - \Theta^4].$$

The output signal of the coordinate meter is equal to

$$\tilde{x}(t) = x(t) + x_{\text{fluct}}(t),$$

where $x^{\text{meter}}(t)$ is the additive noise of the meter. Hence

$$\begin{aligned}\tilde{x}_\omega(\omega) &= x_{D\omega}(\omega) + x_\omega^{\text{meter}}(\omega) \\ &= x_\omega^{\text{signal}}(\omega) + X_\omega(\omega) + x_\omega^{\text{meter}}(\omega),\end{aligned}$$

and SNR is equal to

$$\frac{s}{n} = \int_{-\infty}^{\infty} \frac{|x_\omega^{\text{signal}}(\omega)|^2}{S(\omega)} \frac{d\omega}{2\pi}, \qquad \text{(E.2)}$$

where $S(\omega)$ is the spectral density of the total noise $X_\omega(\omega) + x_\omega^{\text{meter}}(\omega)$.

References

[1] K.S. Thorne, in: 300 years of gravitation, eds. S.W. Hawking and W. Israel (Cambridge Univ. Press, Cambridge, 1987) p. 330.

[2] A. Abramovitch et al., Science 256 (1992) 325.

[3] A. Brillet et al., in: The Detection of Gravitational Waves, ed. D.G. Blair (Cambridge Univ. Press, Cambridge, 1991), p. 369.

[4] D. Nicholson et al., Phys. Lett. A 218 (1996) 175.

[5] V.B. Braginsky and F.Ya. Khalili, Phys. Lett. A 218 (1996) 167.

[6] S.P. Vyatchanin and A.B. Matsko, JETP 83 (1996) 690.

[7] V.B. Braginsky, Yu.I. Vorontsov and F.Ya. Khalili, Sov. Phys.-JETP 46 (1977) 705.

[8] B.J. Meers, Phys. Rev. A 38 (1988) 2317

[9] B. Meers and N. MacDonald, Phys. Rev. A 40 (1989) 3754.

[10] V.B. Braginsky et al., Sov. Phys. Pisma JETP 10 (1972) 157.

[11] V.B. Braginsky, V.P. Mitrofanov and S.P. Vyatchanin, Rev. Sci. Instr. 65 (1994) 3771.

[12] V.B. Braginsky and F.Ya. Khalili, Quantum Measurement, ch. VI, ed. K.S. Thorne (Cambridge Univ. Press, Cambridge, 1992).

[13] V.B. Braginsky, V.P. Mitrofanov and K.V. Tokmakov, Phys. Lett. A 218 (1996) 164.

[14] V.B. Braginsky, M.L. Gorodetsky, V.S. Iltchenko and S.P. Vyatchanin, Phys. Lett. A A (1993) 244;
I.A. Bilenko, E.N. Ivanov, M.E. Tohar and D.G. Blair, Phys. Lett. A 211 (1996) 136.

[15] A.V. Syrtsev and F.Ya. Khalili, Zh. Eksp. Teor. Fiz. 106 (1994) 744;
S.P. Vyatchanin, E.A. Zubova and A.B. Matsko, Opt. Comm. 109 (1994) 492.

30 June 1997

PHYSICS LETTERS A

ELSEVIER

Physics Letters A 231 (1997) 38–46

Heisenberg microscope and quantum variation measurement

S.P. Vyatchanin [1], A.Yu. Lavrenov

Department of Molecular Physics and Physics Measurements, Faculty of Physics, Moscow State University, Moscow 119899, Russian Federation

Received 25 March 1997; accepted for publication 14 April 1997
Communicated by V.M. Agranovich

Abstract

We demonstrate taking the Heisenberg microscope as an example that the standard quantum limit for registration of force can be overcome in a quantum coordinate measurement. We propose to vary the distance between the diffraction slit and detector plane during measurement so that one can measure a linear combination of coordinate and back action momentum transfered to the probe mass in accordance with the uncertainty principle. Changing the distance in a special way enables one to exclude the influence of the back action fluctuations, thus implementing the idea of a quantum variation measurement. © 1997 Elsevier Science B.V.

PACS: 03.75
Keywords: Heisenberg microscope; Quantum measurement; QND measurement

1. Introduction

Quantum noise in a mechanical displacement meter is a key problem in interferometric gravitational-wave antennae (the LIGO project) and in some other fundamental experiments. In a continuous coordinate measurement the back action noise of the meter is responsible for the limit of sensitivity [1–4] known as the standard quantum limit. For the force having the form

$$F_s = F\sin(\omega_F t), \qquad 0 \leqslant t \leqslant 2\pi/\omega_F, \tag{1}$$

acting on a free mass m during a time $T = 2\pi/\omega_F \ll 2\pi/\omega_m$, the standard quantum limit is equal to

$$F_{\mathrm{SQL}} \simeq \sqrt{m\hbar\omega_s^2/T}. \tag{2}$$

Let us consider a simplified example to illustrate why the standard quantum limit appears: a constant signal force acts on a free probe mass during time T and one quickly measures the coordinate of the mass twice: at $t = 0$ (the result is x_1) and at $t = T$ (the result is x_2). Quickly means that the time τ of each measurement

[1] E-mail: vyat@mol.phys.msu.su.

PII S0375-9601(97)00291-0

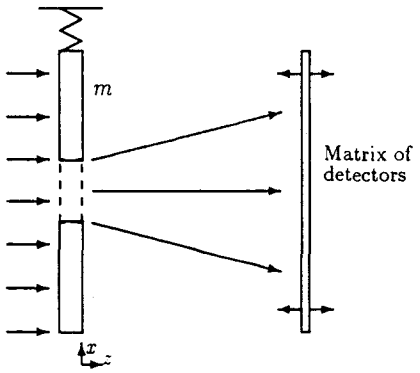

Fig. 1. Scheme of the Heisenberg microscope. The matrix of detectors (detector plane) can move along the z-axis, being parallel to the slit.

is sufficiently small: $\tau \ll T$. The difference x_- between these values allows one to register the signal force. It consists of three terms: $x_- = x_1 - p_1 T/m - x_2$ where p_1 is the back action momentum transfered to the probe mass during the first measurement. The second measurement of the coordinate x_2 can be made with a very small error and conversely the errors of x_1 and p_1 are dependent in accordance with the uncertainty principle: $\Delta x_1 \Delta p_1 \geqslant \hbar/2$. Therefore the error of the measurement of x_- is restricted by the standard quantum limit: $\Delta x_- \simeq \hbar T/m$.

A force measurement with an error of less than F_{SQL} is known to be theoretically possible in continuous coordinate measurement if the noise of the meter is correlated in a special way [2,3] (however, no recipe has been proposed how to obtain the required correlation). A possible way to overcome the standard quantum limit is also to use a modulated pump [5], a pump in a frequency anticorrelated state [6]. Another way is to prepare a pump in a squeezed state [7], however, this squeezing should have a special spectral dependence and it is not clear how this can be realized.

Applying the idea of quantum variation measurement to an optical coordinate meter, it was shown [8–10] that the standard quantum limit can be overcome even with a coherent nonmodulated pump – with no squeezed states, photon number states or any other nonclassical states. To do this one has to use a meter measuring a combination of the coordinate and the back action momentum.

If for the example discussed above, during the first measurement one measures a linear combination $(x_1 + kp_1)$ (k is a constant) and during the second measurement the coordinate x_2 (as before with a small error), then the difference x_- is $x_- = x_1 + kp_1 - p_1 T/m - x_2$. It is easy to see that the constant k can be chosen in a proper way ($k = T/m$) to exclude information about p_1. In this case there is no restriction and the standard quantum limit can be overcome. In Section 2 we present the analysis of this meter for a continuous measurement as a set of instantaneous ones.

A well known example of a coordinate meter is the Heisenberg microscope [11] described in many quantum mechanics textbooks. Despite the fact that the Heisenberg microscope is a *gedanken* scheme which cannot be realized (at least at present) in a laboratory, it is very illustrative and convenient for analysis. In this paper we consider a variant of the Heisenberg microscope with a light beam (the traditional scheme involves an electron beam, however, the difference is not essential).

Let a coherent plane e.m. wave, traveling along the z-axis, diffract on a slit in the probe mass m of a lossless mechanical oscillator, having a frequency ω_m, movable only along the x-axis in the plane $z = 0$ (see Fig. 1). The matrix of photodetectors is placed parallel to the slit plane and in the traditional scheme it is placed close to the slit. Registering the maximum photo count "spot", one can measure the x-coordinate of the slit and therefore the action of the small signal force. Due to the diffraction, each photon transfers the random

x-momentum to the slit – this is the mechanism of the fluctuational back action.

In this paper we demonstrate the possibility in principle to overcome the standard quantum limit for the force in the Heisenberg microscope: one should change the distance between the slit and the detector plane during the measurement. In this case a linear combination of coordinate and back action momentum is measured. Thus one can ignore the back action fluctuations and perform a quantum variation measurement.

In the analysis below we limit the measurement time T to the duration of the signal force action. This is closer to the experimental situation than an unlimited time of measurement. In Section 3 we present a rigorous analysis of the Heisenberg microscope.

2. The quantum variation measurement

In this section we illustrate the possibility to overcome the standard quantum limit in a continuous measurement using a meter sensitive to a linear combination of coordinate and back action momentum. It is worth noting that the meter described below is a simplified one and slightly differs from the Heisenberg microscope. In the next section we discuss the difference between this meter and the Heisenberg microscope.

Let us divide the measurement time $[0,T]$ into n small equal intervals $\tau \ll 2\pi/\omega_m$: $0, t_1, t_2, \dots t_j, \dots t_n$; $t_{j+1} - t_j = \tau$. During each of them the back action momentum $\hat{p}_j$ transfers to the probe mass; the operators $\hat{p}_j$ are independent of each other (in the limit $\tau \to 0$ this means "white" back action noise). It is essential that the meter measures not the coordinate $\hat{x}_j$ but the linear combination $\hat{q}_j = \hat{x}_j + a_j\hat{p}_j$ where the coefficients a_j can be chosen different for each interval. The uncertainties Δx_j^2 and Δp_j^2 are related to each other in accordance with the Heisenberg principle: $\Delta x_j^2 \Delta p_j^2 \geqslant \hbar^2/4$. The expressions for $\hat{q}_j$, measured on the jth interval, are

$$
\begin{aligned}
\hat{q}_1 &= x_{s1} + \hat{x}_{01} + \hat{x}_1 + K(t_1)\hat{P}_0 + a_1\hat{p}_1,\\
\hat{q}_2 &= x_{s2} + \hat{x}_{02} + \hat{x}_2 + K(t_2)\hat{P}_0 + K(t_2 - t_1)\hat{p}_1 + a_2\hat{p}_2,\\
\hat{q}_3 &= x_{s3} + \hat{x}_{03} + \hat{x}_3 + K(t_3)\hat{P}_0 + K(t_3 - t_1)\hat{p}_1 + K(t_3 - t_2)\hat{p}_2 + a_3\hat{p}_3, \qquad \dots,\\
\hat{q}_j &= x_{sj} + \hat{x}_{0j} + \hat{x}_j + K(t_j)\hat{P}_0 + K(t_j - t_1)\hat{p}_1 + K(t_j - t_2)\tau)\hat{p}_2 + \dots + a_j\hat{p}_j, \qquad \dots,\\
\hat{q}_n &= x_{sn} + \hat{x}_{0n} + \hat{x}_n + K(t_n)\hat{P}_0 + K(t_n - t_1)\hat{p}_1 + K(t_n - t_2)\tau)\hat{p}_2 + \dots + a_n\hat{p}_n. \qquad (3)
\end{aligned}
$$

Here $\hat{x}_{sj} = \int_0^{j\tau} F_s(t)K(j\tau - t)\,dt$ is the displacement caused by the signal force F_s, the function $K(t) = (m\omega_m)^{-1}\sin\omega_m t$ describes the action of the external force on the probe oscillator, $\hat{x}_{0j} = \hat{X}_0\cos\omega_m j\tau$, $\hat{X}_0$ and $\hat{P}_0$ are the initial coordinate and momentum.

To register a signal force one should measure the value $B = \sum_0^n \Phi_j\hat{q}_j$, where the coefficients Φ_j should be defined to maximize the signal-to-noise ratio. From the system of equations (3) one can easily obtain (by summing the columns) that the back action momenta $\hat{p}_j$ can be excluded from the value B under the following conditions (on the right side the same formulas in the limit $\tau \to 0$ are presented),

$$
\Phi_k a_k + \sum_k^n \Phi_j K((j-k)\tau) = 0, \qquad \Phi(t)a(t) + \int_t^T dt_1\,\Phi(t_1)K(t_1 - t) = 0. \qquad (4)
$$

To exclude the influence of the initial conditions one should additionally assume

$$
\sum_0^n \Phi_j\cos\omega_m j\tau = 0, \qquad \int_0^T dt\,\Phi(t)\cos\omega_m t = 0, \qquad \sum_0^n \Phi_j K(j\tau) = 0, \qquad \int_0^T dt\,\Phi(t)K(t) = 0. \qquad (5)
$$

In this case the sensitivity is limited only by the measurement error (operator $\hat{x}$) that monotonically decreases with increasing meter power W (in the Heisenberg microscope it is the power of the transmitted beam W). As a result, the minimal registered force $F_{\min}$ is much smaller than the standard quantum limit for the force F_{SQL} (achieved at an optimal power W_{SQL}),

$$F_{\min} = F_{\mathrm{SQL}}\sqrt{W_{\mathrm{SQL}}/W}. \tag{6}$$

It is worth noting that strictly speaking one should not simply exclude the back action momenta p_j but find the optimal coefficients $a_{j,\mathrm{opt}}$ at which ΔB^2, containing the combinations of the independent uncertainties Δx_j^2 and Δp_j^2, is minimized. However, the conditions obtained above are more obvious and they asymptotically approach the precise conditions in the practically interesting limit of strong back action ($W \gg W_{\mathrm{SQL}}$).

3. The analysis of the Heisenberg microscope

First let us consider the traditional scheme when the plane of detectors is close to the slit (i.e. the distance z between them is small: $z \ll d^2/\lambda$, where d is the width of the slit and λ is the wave length of the incident light). It seems natural that in order to get information about the coordinate of the slit, one has to measure $Q = \int x\,\mathrm{d}x\,\mathrm{d}y\; P_z / \int \mathrm{d}x\,\mathrm{d}y\; P_z$ where P_z is the z-component of the Poynting vector $\boldsymbol{P} = \boldsymbol{E} \times \boldsymbol{H}/4\pi$. The integration is in the plane $z = 0$. The error of measurement is caused by the vacuum fluctuations of electrical ($\boldsymbol{E}_{\mathrm{vac}}$) and magnetic ($\boldsymbol{H}_{\mathrm{vac}}$) fields, which should be added to the mean fields $\langle \boldsymbol{E} \rangle$ and $\langle \boldsymbol{H} \rangle$. Keeping the cross terms ($\langle \boldsymbol{E} \rangle \times \boldsymbol{H}_{\mathrm{vac}}$) and ($\boldsymbol{E}_{\mathrm{vac}} \times \langle \boldsymbol{H} \rangle$) in the formula for $\boldsymbol{P}_z$ one can obtain an expression for the operator $\hat{x}$ describing the error of measurement of the coordinate (we consider Gaussian slit with transparency coefficient $\sim \exp\Delta(k_x^2 x^2/2)$, see the Appendix),

$$\hat{x} = -\mathrm{i}\sqrt{\frac{\hbar\omega_0}{4\pi W \Delta k_x^2}} \int_{-\omega_0}^{\infty} \mathrm{d}\Omega\, [a(\Omega)\mathrm{e}^{-\mathrm{i}\Omega t} - a^+(\Omega)\mathrm{e}^{\mathrm{i}\Omega t}]. \tag{7}$$

Here ω_0 and W are the mean frequency and mean power of the transmitted beam, c is the speed of light, the annihilation and creation operators $a(\Omega)$ and $a^+(\Omega)$ describe the vacuum fluctuations of the e.m. fields, their commutators are $[a(\Omega), a^+(\Omega')] = \delta(\Omega - \Omega')$ and the averages are $\langle a(\Omega)a^+(\Omega')\rangle = \delta(\Omega - \Omega')$, $\langle a^+(\Omega)a(\Omega')\rangle = 0$.

The force F_x, acting in the x-direction, is equal to $F_x = -\int \mathrm{d}x\,\mathrm{d}y\; P_x$. Within the same approximation as above one can obtain the operator of the fluctuational back action force $\hat{F}$,

$$\hat{F} = \sqrt{\frac{\hbar\Delta k_x^2 W}{4\pi\omega_0}} \int_{-\omega_0}^{\infty} \mathrm{d}\Omega\, [a(\Omega)\mathrm{e}^{-\mathrm{i}\Omega t} + a^+(\Omega)\mathrm{e}^{\mathrm{i}\Omega t}]. \tag{8}$$

The fluctuation operators $\hat{x}$ and $\hat{F}$, in accordance to the uncertainty principle, can not be decreased simultaneously because they do not commute: $[\hat{x}(t), \hat{F}(t')] = -\mathrm{i}\hbar\delta(t - t')$. With increasing power W, the measurement error decreases, $\hat{x} \sim 1/\sqrt{W}$, and the back action increases, $\hat{F} \sim \sqrt{W}$. This leads to the limitation of the measurement error to the force by the standard quantum limit (2).

However, the situation is radically different if there is a possibility to vary the distance z between the diffractional slit and the plane of detectors during the time of measurement. In the case $z \neq 0$, the effective cross sections of the beam increase and at first sight the error of the coordinate measurement is likely to increase too. However, we would like to emphasize that in this case one measures not the coordinate of the mass, as in the standard scheme, but a linear combination of the coordinate and the back action momentum. It is easy to obtain that in the case $z \neq 0$, the operator $\hat{x}$ should be replaced with the operator $\hat{q} = \hat{x} - (zc/W)\hat{F}$, as in the

meter analyzed in the previous section. This gives the possibility to subtract the back action from the observed value and the standard quantum limit can be overcome.

These equations should be added to the equation for the coordinate X of a mechanical oscillator,

$$\ddot{X} + 2\delta\dot{X} + \omega_m^2 X = \frac{F_s + \hat{F}}{m}. \tag{9}$$

Here $\dot{X}$ is the time derivative of the coordinate, F_s is a signal force, $\delta = W\Delta k_x^2/4m\omega_0^2$ is the coefficient of diffraction friction due to the light beam. The value of this friction depends on the diffraction angle (see the Appendix).

The full expression for the measured value Q is (see the Appendix)

$$Q = \frac{\int x\,dx\,dy\,(E_y H_x^* + \text{c.c.})}{\int dx\,dy\,(\langle E_y\rangle\langle H_x^*\rangle + \text{c.c.})} = X(t) + \dot{X}(t)\frac{c\Delta k_x^2 z(t)}{\omega_0^2} + \hat{x}(t) - \frac{z(t)c}{W}\hat{F}. \tag{10}$$

In experiment one measures B,

$$B = \int_0^T dt\,\Phi(t)Q(t) \tag{11}$$

trying to choose functions $\Phi(t)$ in a proper way to maximize the signal-to-noise ratio.

It is important that the two functions $\Phi(t)$ and the distance $z(t)$ between the slit and the plane of detectors can be changed during the measurement so that terms containing $\hat{F}$ can be excluded. For this, the following condition should be fulfilled (see the Appendix),

$$-\Phi(t)\frac{mz(t)c}{W} + \int_0^t dt_1\,\Phi(t)K(t_1 - t) = 0. \tag{12}$$

The differences between the Heisenberg microscope and the meter described in the previous section are: (a) the existence of the diffraction friction and (b) the presence of a term proportional to the velocity in formula (10). Both of them seem small corrections, however, we surprisingly obtain that condition (12) (exclusion of the influence of the back action) is significantly different from condition (4).

The additional conditions, allowing to one exclude the influence of initial conditions, also differ from (5),

$$\Phi(T)z(T) = 0, \qquad \Phi(T)\dot{z}(T) + \dot{\Phi}(T)z(T) = 0. \tag{13}$$

Under conditions (12), (13) the minimal registered force F_m can be much smaller than the standard quantum limit, however, the sensitivity is limited,

$$F_m = F_{SQL}\sqrt{1/\omega_0 T}, \qquad W_{opt} \simeq W_{SQL}\omega_0 T, \tag{14}$$

where W_{opt} is the required power of transmitted light. This limitation is caused by the diffraction friction (see the Appendix). It leads us to conclude that in spite of the obvious smallness, the radiation friction (as well as the presence of term $\sim \dot{X}$ in (10) – these are closely related) defines the limit of accuracy of this measurement scheme.

It should be noted that another scheme is possible where the detector plane is kept at rest and in front of the slit (or behind it) there is a lens with focal distance, changed during the measurement time in a proper way. We do not consider this scheme in detail because, in our opinion, both variants are the *gedanken* experiments, and the one considered above is more illustrative and convenient for analysis.

4. Conclusion

It is worth noting that the described procedure is not a quantum nondemolition (QND) measurement. The measured value B gives little information about the coordinate, the momentum or any combination of these. These values are strongly perturbed by the measuring device when $W \gg W_{SQL}$ – in accordance with the uncertainty principle. Indeed, during measurement, white noise with a constant intensity acts on the probe oscillator. Therefore we can not find any QND variable of a mechanical system. However, this procedure allows one to exclude the influence of the back action fluctuations and only *variations of the coordinate* caused by the signal force are registered. We propose to call this kind of measurement *quantum variation measurements*.

It is interesting that similar results were obtained for an optic meter [8–10]: the probe mass is a mirror from which a perpendicularly incident beam is reflected (the mirror can move along the direction of beam). The fluctuations of the phase of the wave define the error of the coordinate measurement (the analog of $\hat{x}$ above) and the back action mechanism is the fluctuations of the light pressure force (the analog of $\hat{F}$ above). In the reflected wave one has to measure the especially chosen quadrature component, which is a linear combination of the phase (i.e. $\hat{x}$) and the amplitude (i.e. $\hat{F}$) components. It allows one to exclude the back action from the measured value. For this meter the obtained formulas (12), (13) and (14) are the same except for the difference of notations (in Ref. [9] formula (4) was given incorrectly).

Both these schemes do not require any preliminary preparation of the incident light or use of nonclassical states: a coherent nonmodulated light beam is sufficient. In case of an optic meter the reflected wave is squeezed – it corresponds to the correlation of the phase and amplitude components. In the Heisenberg microscope it is the same: the terms proportional to $[a(\Omega) + a^{+}(-\Omega)]$ and $i[a(\Omega) - a^{+}(-\Omega)]$ describe the amplitude and phase fluctuations of the incident wave respectively and in the transmitted wave they are correlated – which indicates squeezing. This squeezing is not usual: the squeezing in the spectral component of the quadrature amplitude depends on the spectral frequency. The measurement procedure in both schemes should be modified to register such squeezing.

The squeezing means that in the output wave there is a variable defined with a small uncertainty. Trying to relate the quantum variation measurement with the QND measurement, one can claim this variable is a QND one. However, it should be emphasized that this "QND" variable applies to the whole system: the mechanical oscillator plus meter (light beam), but not to just the mechanical system as in orthodox QND measurements [2,3]. These speculations allow one to consider a quantum variation measurement as a generalized QND measurement.

In both of these schemes we observe the possibility to transform a pure coordinate meter into a correlated meter, measuring a linear combination of coordinate and back action force – by only a modification of the procedure of output wave registration. Our opinion is that this is a general property of all coordinate meters.

Acknowledgement

We acknowledge V.B. Braginsky and D.N. Klyshko for fruitful discussions. This work is supported by the Russian Foundation of Fundamental Research (grant 96-02-16319-a) and by the USA National Science Foundation (grant PHY-9503642).

Appendix

Let a plane coherent wave, traveling along the z-axis and polarized along y-axis, be perpendicularly incident on a Gaussian slit, of the which transmission coefficient depends on the transverse coordinate as $\sim \exp(-\Delta k_x^2 x^2/2 - \Delta k_y^2 y^2/2)$. Below we use $\Delta k_y \ll \Delta k_x$. Then the transmitted wave will be a Gaussian beam

and its field is described by the y-component of the vector-potential $\langle A_y \rangle$ (we assume that the scalar potential is zero),

$$\langle A_y \rangle = \sqrt{\frac{2Wc}{\omega_0^2} \frac{\Delta k_x \Delta k_y}{(1+\mathrm{i}\alpha_x)(1+\mathrm{i}\alpha_y)}} \times \exp\left(-\mathrm{i}\omega_0\left(t-\frac{z}{c}\right) - \frac{\Delta k_x^2 (x-X)^2}{2(1+\mathrm{i}\alpha_x)} - \frac{\Delta k_y^2 y^2}{2(1+\mathrm{i}\alpha_y)}\right) + \text{c.c.} \tag{15}$$

Here $\alpha_{x,y} = \Delta k_{x,y}^2 zc/2\omega_0$, X is the coordinate of the slit.

To this field should be added the vacuum fluctuation field of the same polarization which is described by the usual expression for the y-component of the vector-potential $A_{\mathrm{vac},y}$,

$$A_{\mathrm{vac},y} = \int_0^\infty \sqrt{\frac{\hbar c^2}{\omega}} \frac{\mathrm{d}\boldsymbol{k}}{2\pi} b(\boldsymbol{k}) \exp(-\mathrm{i}\omega t + \mathrm{i}\boldsymbol{k}\cdot\boldsymbol{r}) + \text{h.c.}, \tag{16}$$

where $b(\boldsymbol{k})$ and $b^+(\boldsymbol{k})$ are annihilation and creation operators obeying commutation relations $[b(\boldsymbol{k}), b^+(\boldsymbol{k}')] = \delta(k_x - k_x')\delta(k_y - k_y')\delta(k_z - k_z') = \delta(\boldsymbol{k} - \boldsymbol{k}')$. The averages are $\langle b(\boldsymbol{k}) b^+(\boldsymbol{k}') \rangle = \delta(\boldsymbol{k} - \boldsymbol{k}')$, $\langle b^+(\boldsymbol{k}) b(\boldsymbol{k}') \rangle = 0$.

One can define the coordinate of the slit by the measurement of

$$Q = \frac{\int x \,\mathrm{d}x\,\mathrm{d}y\, P_z}{\int \mathrm{d}x\,\mathrm{d}y\, P_z}, \tag{17}$$

where P_z is the z-component of the Poynting vector $\boldsymbol{P} = \boldsymbol{E} \times \boldsymbol{H}/4\pi$. Keeping only linear terms proportional to $\sim E_{\mathrm{vac}}$ and $\sim H_{\mathrm{vac}}$ one can find that the error of the measurement $\hat{x}$ is equal to

$$\hat{x} = -\frac{\int x \,\mathrm{d}x\,\mathrm{d}y\, (\langle E_y \rangle H_{\mathrm{vac},x} + E_{\mathrm{vac},y} \langle H_x \rangle \,\mathrm{d}t)}{\int \mathrm{d}x\,\mathrm{d}y\, \langle E_y \rangle \langle H_x \rangle}.$$

Here $\langle E_y \rangle$ and $\langle H_x \rangle$ are the mean values of the y-component of the electrical field and the x-component of the magnetic field respectively, $E_{\mathrm{vac},y}$ and $H_{\mathrm{vac},x}$ are the same components of the fields of quantum vacuum fluctuations. The integration is over the plane $z = 0$. The calculations give formula (7) for $\hat{x}$, where the operators $a(\Omega)$ are equal to

$$a(\Omega) = -\sqrt{\frac{1}{2\pi c \Delta k_x^3 \Delta k_y}} \int \left(\sqrt{\frac{\omega}{\omega_0}} + \sqrt{\frac{\omega_0}{\omega}}\right) k_x \,\mathrm{d}k_x\,\mathrm{d}k_y\,\mathrm{d}k_z\, b(\boldsymbol{k}) \left(\frac{k^2 + k_z^2}{2k}\right) \left[\frac{k^2}{2\Delta k_x^2} \frac{k^2}{2\Delta k_y^2} \frac{\mathrm{i}(k^2 + k_z^2) z}{2k} \left(\frac{c}{\omega} - \frac{c}{\omega_0}\right)\right] \tag{18}$$

Here $|\boldsymbol{k}|^2 = k^2 = k_x^2 + k_y^2 + k_z^2$, $\omega = kc$, $\Omega = \omega - \omega_0$. In this paper we assume $\sqrt{\omega/\omega_0} + \sqrt{\omega_0/\omega} = 2$.

The transmitted beam induces the force $-\int \mathrm{d}x\,\mathrm{d}y\, (P_x)$ acting on the mass in the x-direction. The mean value of this force is equal to zero and its fluctuational part is $\hat{F} = -\int \mathrm{d}x\,\mathrm{d}y\, (\langle E_y \rangle H_{\mathrm{vac},z} + E_{\mathrm{vac},y} \langle H_z \rangle)$. From this formula expression (8) is obtained.

The diffraction friction is a classical (not a quantum) effect and to calculate it one should take into account only mean fields. Let us assume that the slit moves uniformly with velocity V along the x-direction. In the frame of reference where the slit is at rest the incident wave moves not perpendicularly to the slit but at a small angle $\sim V/c$ and one can write down the expression for the transmitted wave. Returning to the laboratory

reference frame one can obtain the formula for the y-component of the vector-potential $\langle A_y\rangle$ (here and below we keep only terms linear to $\sim V/c$ and drop the terms $\sim (V/c)^2$),

$$\langle A_y\rangle = \sqrt{\frac{2Wc}{\omega_0^2}\frac{\Delta k_x \Delta k_y}{(1+\mathrm{i}\alpha_x)(1+\mathrm{i}\alpha_y)}} \times \exp\left(-\mathrm{i}\omega_0(t-z/c) - \frac{\Delta k_x^2 (x - X - V(t-z/c))^2}{2(1+\mathrm{i}\alpha_x)} - \frac{\Delta k_y^2 y^2}{2(1+\mathrm{i}\alpha_x)}\right) + \text{c.c.} \tag{19}$$

Calculating the fields $\langle E_y\rangle$, $\langle H_z\rangle$ one can obtain the expression for the force of the diffraction radiation proportional to V,

$$F_x = -\int \mathrm{d}x\,\mathrm{d}y\,(\langle E_y\rangle\langle H_z^*\rangle + \text{c.c.}) = \frac{W\Delta k_x^2}{2\omega_0^2} V = 2m\delta V. \tag{20}$$

This formula gives an expression for the coefficient δ of the diffraction friction.

To obtain the term proportional to V in formula (10) let us substitute the expression for the fields $\langle E_y\rangle$, $\langle H_x\rangle$ into (17). Then one obtains

$$\frac{\int x\,\mathrm{d}x\,\mathrm{d}y\,(\langle E_y\rangle\langle H_x^*\rangle + \text{c.c.})}{\int \mathrm{d}x\,\mathrm{d}y\,(\langle E_y\rangle\langle H_x^*\rangle + \text{c.c.})} = X + \frac{c\Delta k_x^2 z}{\omega_0^2}\dot{X}. \tag{21}$$

We see that this effect and the diffraction friction are close to each other and they are derived from the same basis formula (19).

To obtain formulas (12) and (13) let us express $\hat{F}$ from (8) and substitute it into (10),

$$Q = \hat{x}(t) + X_s(t) + X(t) + \dot{X}(t)\frac{c\Delta k_x^2 z(t)}{\omega_0^2} - \frac{mz(t)c}{W}(\ddot{X} + 2\delta\dot{X} + \omega_m^2 X). \tag{22}$$

Using that $\delta = W\Delta k_x^2/4m\omega_0^2$ one can simplify this formula, substitute it into (11) and integrate by parts,

$$B = \int_0^T \mathrm{d}t\,\Phi(t)\left(\hat{x}(t) + X(t) - \frac{mz(t)c}{W}(\ddot{X} - 2\delta\dot{X} + \omega_m^2 X)\right)$$

$$= \int_0^T \mathrm{d}t\,\Phi(t)[\hat{x}(t) + X_s(t)] + \int_0^T \mathrm{d}t\,X(t)\{\Phi(t) - [\ddot{\phi}(t) + 2\delta\dot{\phi}(t) + \omega_m^2\phi(t)]\} - 2\delta\phi X\big|_0^T - \phi\dot{X}\big|_0^T + \dot{\phi}X\big|_0^T,$$

$$\phi(t) = \frac{mz(t)c}{W}\Phi(t). \tag{23}$$

Requiring the second integral in the right-hand side of (23) to be equal to zero one can obtain the differential equation, of which the solution is condition (12). Conditions (13) are obtained if one requires the three last terms to be equal to zero. Here we use that $\phi(0) = \dot{\phi}(0) = 0$ (this follows from (12) if the function Φ is limited on the interval $[0,T]$ and $\Phi(0) = \Phi(T) = 0$). It is worth emphasizing that X in (23) includes the back action disturbance and also the free evolution due to the nonzero initial conditions.

In this case the value B is equal to $B = \int_0^T \mathrm{d}t\,\Phi(t)[\hat{x}(t) + X_s(t)]$. The measurement error $\hat{x}$ decreases with increasing W and the signal displacement X_s does not depend on W until the diffraction friction coefficient (which is proportional to W) is small. In the free mass approximation this means $\delta T \ll 1$. In the opposite case $X_s \simeq F_s/m\delta T \sim 1/W$ decreases with increasing W faster than the error $\hat{x} \sim 1/\sqrt{W}$. Therefore the signal-to-noise ratio has a maximum about $\delta T \simeq 1$ and formulas (14) are obtained.

References

[1] V.B. Braginsky, Zh. Eksp. Teor. Fiz. 53 (1967) 1436 [Sov. Phys. JETP 26 (1968) 831]; Physical experiments with probe bodies (Nauka, Moscow, 1970) p. 50 [in Russian];
V.B. Braginsky and A.B. Manukin, Measurements of weak forces in physics experiments (University of Chicago Press, Chicago, 1977).
[2] Yu.I. Vorontsov, Theory and methods of macroscopic measurement (Nauka, Moscow, 1989) p. 200 [in Russian].
[3] V.B. Braginsky and F.Ya. Khalili, in: Quantum measurement, ed. K.S.Thorne (Cambridge Univ. Press, Cambridge, 1992) p. 106.
[4] Yu.I. Vorontsov, Usp. Fiz. Nauk 164 (1994) 101 [Phys. Usp. 37 (1994) 81].
[5] A.V. Syrtsev and F.Ya. Khalili, Zh. Eksp. Teor. Fiz. 106 (1994) 744 [Sov. Phys. JETP 79 (1994) 409].
[6] V.B. Braginsky and F.Ya. Khalili, Zh. Eksp. Teor. Fiz. 94 (1988) 151 [Sov. Phys. JETP 67 (1988) 84].
[7] M.T. Jaekel and S. Reynaud, Europhys. Lett. 13 (1990) 301.
[8] S.P. Vyathanin, E.A. Zubova and A.B. Matsko, Opt. Commun. 109 (1994) 492.
[9] S.P. Vyathanin and E.A. Zubova, Opt. Commun. 111 (1994) 303.
[10] S.P. Vyathanin and A.B. Matsko, Zh. Eksp. Teor. Fiz. 109 (1996) 1873 [Sov. Phys. JETP 82 (1996) 1007]; Zh. Eksp. Teor. Fiz. 110 (1996) 1253 [Sov. Phys. JETP 83 (1996) 690].
[11] W. Heisenberg, Z. Phys. 4 (1925) 879;
L.I. Mandestam, Lectures on optics, the theory of relativity and quantum mechanics (Nauka, Moscow, 1972) [in Russian];
D.I. Blokhintsev, The basis of quantum mechanics (Nauka, Moscow, 1983) pp. 63–83 [in Russian].